

**MICROBIAL ELECTROCHEMISTRY APPLICATIONS FOR  
NUTRIENT RECOVERY AND ORGANIC DETECTION IN  
WASTEWATER TREATMENT**

MICROBIAL ELECTROCHEMISTRY APPLICATIONS FOR  
NUTRIENT RECOVERY AND ORGANIC DETECTION IN  
WASTEWATER TREATMENT

By:

PENGYI YUAN, B. Eng.

A Thesis Submitted to the School of Graduate Studies  
in Partial Fulfillment of the Requirements for the Degree  
Master of Applied Science

McMaster University

© Copyright by Pengyi Yuan, April 2017

McMaster University, Hamilton, Ontario

MASTER OF APPLIED SCIENCE, Civil Engineering, 2017

TITLE: Microbial electrochemistry applications for nutrient recovery and organic detection in wastewater treatment

AUTHOR: Pengyi Yuan, B. Eng

SUPERVISOR: Dr. Younggy Kim

NUMBER OF PAGES: xi, 59

## Abstract

This thesis presents research work on microbial electrochemistry applications for phosphorus recovery from real wastewater and bioanode sensor development. Phosphorus is a valuable but limited resource which is essential for land fertilizers. Recovering phosphorus using microbial electrolysis cells has been emphasized in wastewater treatment research. Stainless steel mesh (SSM) cathode MECs used in this study showed insufficient phosphorus recovery (68%) because struvite crystals were smaller than the open space between mesh wires (80  $\mu\text{m}$ ). Besides, lack of readily biodegradable substrates in the dewatering centrate resulted in limited electric current generation ( $< 0.2 \text{ A/m}^2$ ) and local pH condition near the cathode. Thus, the following experiments were conducted with stainless steel foil (SSF) cathodes and acetate addition to improve recovery efficiency. Under high electric current density ( $> 2 \text{ A/m}^2$ ), a thick layer of struvite crystals was formed on the SSF cathode and the phosphorus recovery was increased to 96%. These findings prove that MECs can be applied as efficient tools to recover nutrients from real wastewater.

Bioanode sensors can be used for real-time and in-situ assessment of water quality. However, the sensor performances are often limited by the narrow detection range, long analysis time, and hysteresis. In order to overcome the challenges for practical applications, a new operation method consisting of three sequences (Normal Operation, Reset Step, and Test Step) was proposed and examined using MEC-based bioanode sensors. Reset Step can eliminate hysteresis effects and produce accurate linear correlations between the soluble COD (chemical oxygen demand) and electric current. The total analysis time was found to be 3 min or even less. The increased detection range (from 75 to 130 mg-COD/L) was achieved by applying a high applied voltage during Test Step. The demonstrated results indicate that MECs can be used for accurate estimation of biodegradable organics in natural or engineered water systems.

## **Acknowledgements**

Firstly, I want to sincerely thank my supervisor, Dr. Younggy Kim, for all his help and support over the past two years. He has not only been an excellent mentor who keeps providing me challenges and guidance on researches, but also a close friend who inspires me all the time. It was truly a privilege to have such a brilliant person as my supervisor for my master study.

I would like to thank Dr. Brian W. Baetz and Dr. Zoe Li for being my examination committee members. Thanks to Ms. Anna Roberstson, and Ms. Monica Han for their support within the laboratory. Thanks to Mr. Peter Koudys for his assistance on reactor construction. I would also like to thank all my research group mates, Wendy, Jeff, Natalie, Hui, Yousif, and Erin, for all their help and company over the past years.

Last but not least, I would like to thank my parents for their endless belief and support. Their unconditional love and encouragement help me conquer all the challenges and difficulties. I couldn't accomplish more without them.

## Table of Contents

|  |      |
|--|------|
| Abstract.....  | iii  |
| Acknowledgements.....  | iv   |
| List of Figures.....   | viii |
| List of Tables.....  | ix   |
| List of Additional files.....  | x    |
| Declaration of Academic Achievement.....   | xi   |
| 1. Introduction.....   | 1    |
| 1.1 Microbial electrolysis cells.....  | 1    |
| 1.2 Phosphorus recovery using microbial electrolysis cells.....                        | 1    |
| 1.3 Applying microbial electrolysis cell as bioanode sensor for organic detection..... | 2    |
| 1.4 Research objectives.....   | 2    |
| 2. Literature review.....  | 4    |
| 2.1 Phosphorus recovery from nutrient-rich wastewater.....                             | 4    |
| 2.1.1 Phosphorus recovery in microbial fuel cells.....                                 | 4    |
| 2.1.2 Phosphorus recovery in microbial electrolysis cells.....                         | 5    |
| 2.2 Development of bioanode sensor for water quality assessment.....                   | 7    |
| 2.2.1 Methods of organic measurement.....  | 7    |
| 2.2.2 Bioanode sensors based on luminous bacterium.....                                | 8    |
| 2.2.3 Bioanode sensors based on microbial fuel cells.....                              | 8    |

|   |    |
|---|----|
| 2.2.3.2 Bioanode sensors based on microbial electrolysis cells .....                          | 10 |
| 3. Increasing phosphorus recovery from dewatering centrate in microbial electrolysis cells .. | 11 |
| Abstract .....  | 11 |
| 3.1. Introduction.....  | 13 |
| 3.2. Methods.....   | 15 |
| 3.2.1. Reactor design and construction .....  | 15 |
| 3.2.2. Reactor start-up and operation .....   | 17 |
| 3.2.3. Experiment measurement.....  | 19 |
| 3.4. Results and discussion .....   | 20 |
| 3.4.1. SSM cathode for struvite production .....  | 20 |
| 3.4.2. Electric current and COD removal .....   | 22 |
| 3.4.3. Enhanced struvite recovery with SSF and high electric current .....                    | 24 |
| 3.4.4. Energy requirement for struvite production.....  | 26 |
| 3.5. Conclusions.....   | 27 |
| 4. Bioanode sensor for rapid organic detection in water systems.....                          | 29 |
| Abstract .....  | 29 |
| 4.1. Introduction.....  | 30 |
| 4.2. Methods.....   | 32 |
| 4.2.1. Sensor construction and start-up.....  | 32 |
| 4.2.2. Sensor operation.....  | 33 |

|   |    |
|---|----|
| 4.2.3. Experimental measurement.....                                | 34 |
| 4.3. Results and discussions.....                                   | 34 |
| 4.3.1. Bioanode sensor performance without Reset or Test Steps..... | 34 |
| 4.3.2. Effects of $E_{ap}$ on sensor reliability .....              | 36 |
| 4.3.4. Role of Reset Step.....                                      | 37 |
| 4.3.5. Challenges in bioanode sensor applications .....             | 40 |
| 4.4. Conclusions.....   | 41 |
| 5. Conclusions.....   | 42 |
| References.....   | 44 |
| Appendix A: Additional files for Chapter 3 .....                    | 53 |
| Appendix B: High current operation using a microcontroller .....    | 56 |
| Introduction.....   | 56 |
| Methods.....  | 57 |
| Programmed logic description .....                                  | 57 |
| Description of electric connections with PLC .....                  | 58 |
| Results.....  | 59 |



## List of Figures

Figure 3.1 (A) Schematic diagram of MEC constructed with the SSM cathode (5 SSM pieces).

(B) Schematic diagram of MEC with the SSF cathode

Figure 3.2 Electric current generation in MECs with the SSM cathode: (A) effect of the number SSM pieces in Sets A and B; (B) effect of phosphate concentration in Set C

Figure 3.3 Electric current generation in MECs with the SSM cathode: (A) effect of the number SSM pieces in Sets A and B; (B) effect of phosphate concentration in Set C

Figure 3.4 Phosphorus removal and recovery with the SSF cathode (Set D)

Figure 3.5 Electric current generation in during the MEC operation with the SSF cathode (Set D)

Figure 4.1 Sequence of applied voltage in Set 2

Figure 4.2 Correlation between sCOD and electric current at the end the Normal operation (No Reset Step; No Test Step) in Set 1

Figure 4.3 Correlations between sCOD and electric current at the end of Test Step (No Reset Step) in Set 1

Figure 4.4 Correlations between sCOD concentration and electric current with Reset Step in Set2

Figure 4.5 Electric current variation in Sensor 2 during Test Step with and without Reset Step at (A) relatively high sCOD concentration and (B) low sCOD concentration

Figure 4.6 Changes in the sensor correlation with time in Sensor 1 with Rest Step

## List of Tables

Table 3.1 Feed preparation and MEC operation in four experimental sets

Table 3.2 Phosphorus removal and recovery ( $n = 3$ ; mean  $\pm$  standard error)

Table 3.3 COD removal and Coulombic efficiency ( $n = 3$ ; mean  $\pm$  standard error)

Table 4.1 Sensor calibration equations obtained by linear regression from experiments with

Reset Step in Set 2

## List of Additional files

Figure S 1 Dewatering centrate sample

Figure S 2 (A) SSM cathode image after controlled experiment (open circuit) with 2 mM magnesium and 4.5 mM phosphate addition. (B) SSM cathode image after one fed-batch SSM MEC operation with 4.5 mM phosphate addition for Set C

Figure S 3 SEM images of struvite crystals on the SSM cathode after one fed-batch cycle (Set C with initial phosphate concentration of 3.26 mM)

Figure S 4 (A) EDS analysis results for the crystal on the SSM cathode. (B) EDS analysis results for pure struvite (99.999% purity)

Figure S 5 SSF cathode image after 5-day fed-batch SSF MEC operation for Set D

Figure S 6 Operation sequence

Figure S 7 Connections of MEC and LabJack

Table S 1 Recent test results of examining primary clarifier effluents

## **Declaration of Academic Achievement**

This dissertation consists of previously prepared material that is either published or is currently under review for publication in peer-reviewed scientific journals. The author of this dissertation is the primary author on each of these articles. As the primary author, contributions included: experimental design, literature review, collection and analysis of data, and manuscript preparation. The thesis supervisor is the second author on each of these articles. He offered input and expertise during each phase of the research process and manuscript preparation. Chapter 3 has been accepted for publication in the journal *Biotechnology for Biofuels* (Yuan, P. and Kim, Y., 2017. Increasing phosphorus recovery from dewatering centrate in microbial electrolysis cells. *Biotechnology for Biofuels*, 10(1), p.70.). Chapter 4 has been submitted to the journal *Environmental Science: Water Research & Technology* and is currently under review.

# 1. Introduction

## *1.1 Microbial electrolysis cells*

Microbial electrolysis cells (MECs) is a promising bioelectrochemical technology which has presented great potentials in wastewater treatment, bioenergy generation, nutrients recovery, sensor development, heavy metal removal, etc. By applying a small amount of voltage ( $> 0.2\text{V}$ ), organic matters can be oxidized by exoelectrogens at the bioanode, simultaneously water molecules are reduced to hydrogen gases at the cathode (Liu et al. 2005; Logan et al. 2008). In contrast to conventional wastewater treatment, MECs are more sustainable and energy efficient, and also provide solutions to overcome growing wastewater treatment issues.

## *1.2 Phosphorus recovery using microbial electrolysis cells*

Phosphorus is a valuable resource which is essential for land fertilizers (Gilbert 2009). Recovering phosphorus from nutrient-rich wastewater stream has become an emerging topic in wastewater treatment researches. One of the solutions is to recover phosphate along with ammonia from dewatering centrate as struvite ( $\text{MgNH}_4\text{PO}_4 \cdot 6\text{H}_2\text{O}$ ). Accordingly, studies on struvite precipitation always involve adding strong base chemicals because substantially high pH is required to reach oversaturation of struvite (Nancharaiah et al. 2016; El Diwani et al. 2007; Ronteltap et al. 2007; Ryu et al. 2008). In MECs, the cathodic reaction releases hydroxyl ions and creates a local high pH condition. Thus, it is feasible to achieve spontaneous struvite precipitation at the cathode of MECs without dosing strong base chemicals. Despite that the reliability of removing phosphorus

as struvite in MECs had been demonstrated by some studies (Cusick & Logan 2012; Cusick et al. 2014), the recovery efficiency has not been thoroughly investigated.

### ***1.3 Applying microbial electrolysis cell as bioanode sensor for organic detection***

The development of bioanode sensors is an innovative approach for real-time monitoring of biodegradable organics in wastewater treatment. The standard methods for measuring biochemical oxygen demand (BOD) and chemical oxygen demand (COD) are well-accepted, but they are considered slow and complicated. Microbial fuel cells (MFCs) rather than MECs has been widely investigated as a bioanode sensors for organic detection (Kaur et al. 2014; Kumlanghan et al. 2007; Chang et al. 2004). However, its detection range and sensitivity is often limited by internal resistance, microbial efficiency, and data irreproducibility. In two recent studies, MECs has been proven to be a more robust biosensor with a much wide detection range (Quek et al. 2014; Jin et al. 2016). However, the analysis time requirements demonstrated in these two works are still considered not quick enough.

### ***1.4 Research objectives***

The primary goal of this thesis is to provide a clear understanding on two potential applications of microbial electrolysis cell in wastewater treatment: 1) recovering phosphorus as struvite from dewatering centrate in microbial electrolysis cells; 2) applying microbial electrolysis cells as bioanode sensors for organic detection.

In chapter three, we examined dewatering centrate from a local wastewater treatment plant and we also focused on demonstrating complete phosphorus recovery in MECs. To achieve

efficient phosphorus recovery, various cathode configurations (mesh vs. foil types; single vs. multiple pieces) were examined in lab-scale MEC experiments for efficient struvite precipitation. In addition, for effective struvite production, high electric current is desired and thus a readily available organic substrate is necessary for MEC operation. Since dewatering centrate is lacking readily available organic substrates, we studied the effect of electric current generation in MECs on the phosphorus recovery. Finally, the time requirement for struvite precipitation was also investigated in this study.

Chapter four focuses on developing a new operation method to remove hysteresis effects in MEC-based bioanode sensors for accurate and rapid detection of biodegradable organics. The new operation method consisted of three sequences (Normal operation, Reset Step, and Test Step). We first investigated how the sensors performed during Test Step without Reset Step. Then the results were compared with the electric current performances by implementing a high applied voltage (Reset Step) for a short time period (1 min) before Test Step. We examined how the high voltage application can shorten the time requirement for steady-state electric current generation in the bioanode sensor. In addition, we interpreted how the detection range was affected by applied voltages. Finally, the time effect on sensor performance was tested to identify potential challenges for practical applications.

## 2. Literature review

### *2.1 Phosphorus recovery from nutrient-rich wastewater*

#### **2.1.1 Phosphorus recovery in microbial fuel cells**

Phosphorus recovery from nutrient-rich wastewater or synthetic wastewater using microbial fuel cells has been widely studied. In 2011, a group demonstrated the feasibility of microbial fuel cells (MFC) to enable phosphate recovery from digested sewage sludge as struvite (Fischer et al. 2011). Phosphate was released from iron phosphate ( $\text{FePO}_4$ ) contained in digested sewage sludge at a two-chamber MFC cathode due to reduction of iron from ferric to ferrous. Orthophosphate containing supernatant was collected from MFC after up to 21-day operation. Stoichiometric amounts of  $\text{MgCl}_2$  and  $\text{NH}_4\text{OH}$  were added into the filtered supernatant to synthesize struvite. Despite that phosphorus was successfully recovered as land fertilizer, the reactor design and the overall approach was considered to be complicated.

Recovery of phosphorus spontaneously as struvite from swine wastewater using an air-cathode single-chamber microbial fuel cell was discovered by a Japanese research group in 2011 (Ichihashi et al. 2011). They hypothesized that the struvite precipitation was due to a local pH increase near the cathode caused by oxygen reduction reaction. Afterwards, removal and recovery efficiency and its effect on power generation was investigated (Ichihashi and Hirooka 2012; Hirooka and Ichihashi 2013). In their first paper, 70–82% of the phosphorus was removed from the influent and the precipitates observed on the liquid side cathode surface contained phosphorus equivalent of 4.6–27% of the influent. The X-ray diffraction analysis confirmed that the majority of these precipitates were struvite. In the second paper, the effects of the concentration of  $\text{NH}_4$  and Mg were examined using artificial wastewater by conducting a series of experiments with different molar ratios to phosphate concentration. An increasing trend of precipitates was identified as the



concentration of ammonium and magnesium increased. Furthermore, they revealed that the performance of the MFCs could be reduced as precipitates were being produced. These studies proved the feasibility of recovering phosphorus as struvite directly in the cathode chamber of MFC, but the recovery was considered to be non-ideal.

Recently, another research group published a paper on enhanced MFC struvite recovery by the addition of sea salts to urine (Merino Jimenez et al. 2016). Human urine is known to contain rich ammonium and phosphate, which is considered an excellent source for nutrient recovery (Maurer et al. 2006; Larsen et al. 2009). In this study, a commercialized sea salt named SeaMix was proposed as an alternative source of magnesium. Its effect on struvite recovery was demonstrated in contrast to  $MgCl_2$  and artificial sea water. However, they suggested mixing SeaMix with human urine to favour struvite precipitation prior to feeding MFC. The reactor performance was not reduced and, in fact, was enhanced by 10%. In addition, 94% of struvite recovery was achieved and the unit cost was estimated to be lower than  $MgCl_2$  addition.

### **2.1.2 Phosphorus recovery in microbial electrolysis cells**

The microbial electrolysis cell (MEC) is a similar bioelectrochemical system to MFC, which can be also be applied to recover phosphorus as struvite from wastewater. In MEC, microorganisms oxidize organic matters at a significantly lower voltage ( $>0.2V$ ), and energy can be recovered in the form of hydrogen gas instead of electricity. At the MEC cathode, the hydrogen evolution reaction also produces hydroxyl ions and creates a local high pH condition near the cathode surface, which can be utilized to oversaturate struvite in nutrient-rich wastewater, including synthetic wastewater.

The feasibility of struvite precipitation in MEC was first explored in 2012 (Cusick & Logan 2012). In this study, synthetic wastewater containing ammonium phosphate was used and  $MgCl_2$  was selected as magnesium source. The concentration of each component in the feed solution was estimated to mimic those commonly found in anaerobic digester supernatant. Two types of cathode materials were examined in single-chamber MECs, which were stainless steel mesh and stainless steel flat. The resulting mesh cathode achieved phosphate removal ranging from 20% to 40%, which was more efficient than the flat cathode. Scanning electron microscope (SEM) and energy dispersive spectroscopy (EDS) verified that precipitates on the cathode were struvite. In addition, this study demonstrated an increasing removal of phosphate as the applied voltage increased. However, the recovery of phosphate was not estimated. Overall energy efficiency suggests that the energy recovery as hydrogen gas can offset the energy demand for struvite precipitation in MEC.

Struvite precipitation from real anaerobic digester supernatant with a fluidized bed cathode microbial electrolysis cell was demonstrated in 2014 (Cusick et al. 2014). This study examined a two-chamber MEC designed with a fluidized bed to produce suspended particles and prevent scale formation on the cathode surface. The results indicated that the scouring of the stainless steel mesh cathode by fluidized particles can prevent scale accumulation and prolong the reactor operation. Phosphorus removal was evaluated by calculating the difference between total phosphorus in influent and soluble phosphorus in effluent, which ranged from 70 to 85%. The amount of struvite precipitates attached on the cathode surface or the recovery efficiency was not quantified. In contrast to other struvite formation methods based on pH adjustment such as aeration and adding base chemicals, the energy consumption in this experiment from both power supplier and pumping was significantly lower. Additionally, organic matters and ammonium were removed from

supernatant mixed with sodium acetate in the anode chamber. Also, the rates of organic removal and ammonium removal represented a positive correlation with the applied voltage.

Unexpected struvite precipitation was found in the nutrient separation microbial electrolysis cell used to study the energy efficient reconcentration of diluted human urine using ion exchange membranes in bioelectrochemical systems (Tice & Kim 2014). This unexpected finding confirmed the capacity of MECs in term of recovering nutrients from wastewater. Note that the morphology of the struvite precipitates found in this study was different from either of the previous studies (Cusick & Logan 2012; Cusick et al. 2014).

## ***2.2 Development of bioanode sensor for water quality assessment***

### **2.2.1 Methods of organic measurement**

The traditional measurements of biodegradable organics in water quality assessment includes biochemical oxygen demand (BOD) and chemical oxygen demand (COD). BOD is defined as the concentration of oxygen used to biodegrade organic carbon in 5 days (BOD<sub>5</sub>), while COD measures the amount of oxygen needed to oxidize all the organic matters by strong oxidizing agents under acid conditions. In comparison, BOD<sub>5</sub> is considered reliable but slow and requires professional personnel to reduce measurement variability. Even if the COD method is relatively quick and simple, which takes 2 hours, the strong oxidizing capacity of dichromate often overestimates biodegradable organics in samples. However, neither of methods is ideal for real-time and in-situ monitoring of organics in natural or engineered water systems.

Alternative approaches for biodegradable organics measurement is attributed to bacteria, which are known as bioanode sensors. A bioanode sensor is an analytical device which integrates a biological recognition element with a physical transducer to generate a measurable signal proportional to the concentration of the analytes (Jouanneau et al. 2014). In recent years, a large number of bioanode sensors have been developed for water quality assessment. These sensors are mainly used for biodegradable organics monitoring and toxicity monitoring. This thesis focuses on the development of bioanode sensors on biodegradable organics detection.

### **2.2.2 Bioanode sensors based on luminous bacterium**

The types of bioanode sensors can be categorized based on how the bacteria responded to the analyte concentration. The performance of a bioanode sensor based on immobilized luminous bacterium was improved in 2007 (Sakaguchi et al. 2007) in comparison with the previous study (Sakaguchi et al. 2003). Accordingly, the bioluminescence emission intensity is correlated with a carbon source under aerobic conditions. A linear regression ( $R^2 = 0.995$ ) was obtained with reduced response time (25 min). However, the detection range of this approach was limited up to approximately 16 mg/L as BOD. Also, further development of this method was restrained by the complexity of the system.

### **2.2.3 Bioanode sensors based on microbial fuel cells**

Another popular type of bioanode sensor is based on bioelectrochemical systems which include microbial fuel cells (MFCs) and microbial electrolysis cells (MECs). Both systems can oxidize organic matters at the bioanodes and generate electric current signals (Logan et al. 2006; Logan et

al. 2008). Monitored electric current generation at steady state can be correlated to the substrate concentration in the cells.

In recent years, MFC-based bioanode sensors have been widely explored. The performance of a single-chamber MFC was demonstrated in 2009 (Di Lorenzo et al. 2009). The coefficient of determination ( $R^2$ ) was estimated to be 97% while the reactor was fed with synthetic wastewater using glucose as substrate. The detection range of this bioanode sensor was up to 350 mg/L as COD. Furthermore, the reactor proved high data reproducibility and stability over 7 months of operation. Moreover, the effect of distinct factors was investigated to shorten the response time. Among these factors, reducing reactor volume contributed efficiently to the response time. A response time of 40 min was observed when the reactor volume was reduced from 50 mL to 12.6 mL.

Another type of bioanode sensors using submersible MFCs was developed for in-situ monitoring of microbial activity and BOD in groundwater in 2011 (Zhang & Angelidaki 2011). The performance of the bioanode sensors was tested with three types of wastewater: acetate-based synthetic wastewater; glucose-based synthetic wastewater; and primary clarifier effluent. The detection range was from 10 to 250 mg/L as BOD and the reactor was found to be saturated when the substrate concentration was higher than 250 mg/L as BOD. Correlations between current density and BOD concentration of three samples showed high  $R^2$  values (>97%). Regarding the response time, an increasing trend was detected as the substrate concentration was increased. The response time was nearly 0.67 hr for substrate concentration greater than 150 mg/L as BOD.

### 2.2.3.2 Bioanode sensors based on microbial electrolysis cells

Though MFCs have been broadly developed as bioanode sensors, the detection range and response time are often limited by cathode oxygen reduction. To overcome this limitation, exploration of MEC-based bioanode sensors for biodegradable organics has recently emerged.

A study of MEC-based bioanode sensor for biodegradable organics detection was demonstrated in 2014 (Quek et al. 2014). Note that this study focused on detecting low limits for the MEC-based bioanode sensor. Thus, the detection range being investigated was from 10 to 170  $\mu\text{M}$  acetate, equivalent to 0.46 to 7.81 mg/L as COD. Also, the results reproducibly showed a linear relationship between electric current generation and substrate concentration ( $R^2 > 99\%$ ). Additionally, the response time was found to be dependent on the substrate concentration and ranged from 10 min to 120 min.

Volatile fatty acids (VFA) are significant parameters for monitoring anaerobic digestion process, and are also a typical biodegradable organic in wastewater treatment. A recent study has tested a MEC-based bioanode sensor with synthetic wastewater containing varying concentrations of sodium acetate, sodium propionate and sodium butyrate (total VFAs ranges from 0 to 120 mM) (Jin et al. 2016). The results found a linear regression with  $R^2$  equals to 99%. However, the electric current data was constantly collected at 1 hr after a fresh feed instead of at steady state. Moreover, a 10-hr starvation was suggested between each test, which subcutaneously increased analysis time.

### **3. Increasing phosphorus recovery from dewatering centrate in microbial electrolysis cells**

#### ***Abstract***

MECs (microbial electrolysis cells) use bioelectrochemical reactions to remove organic contaminants at the bioanode and produce hydrogen gas at the cathode. High local pH conditions near the cathode can also be utilized to produce struvite from nutrient-rich wastewater. This beneficial aspect was investigated using lab-scale MECs fed with dewatering centrate collected at a local wastewater treatment plant. The main objective was to improve phosphorus recovery by examining various cathode configurations and electric current conditions.

The stainless steel mesh (SSM) cathode was relatively inefficient to achieve complete phosphorus recovery because struvite crystals were smaller (a few to tens of micrometers) than the open space between mesh wires (80  $\mu\text{m}$ ). As a result, the use of multiple pieces of SSM also showed a limited improvement in the phosphorus recovery up to 68% with 5 SSM pieces. Readily available organic substrates were not sufficient in the dewatering centrate, resulting in relatively low electric current density (mostly below 0.2  $\text{A}/\text{m}^2$ ). The slow electrode reaction did not provide sufficiently high pH conditions near the cathode for complete recovery of phosphorus as struvite. Based on these findings, additional experiments were conducted using stainless steel foil (SSF) as the cathode and acetate (12 mM) as an additional organic substrate for exoelectrogens at the bioanode. With the high electric current ( $> 2 \text{ A}/\text{m}^2$ ), a thick layer of struvite crystals was formed on the SSF cathode. The phosphorus recovery increased to 96% with the increasing MEC operation time from 1 to 7 days. With the high phosphorus recovery, estimated energy requirements were

relatively low at 13.8 kWh (with acetate) and 0.30 kWh (without acetate) to produce 1 kg of struvite from dewatering centrate.

For efficient phosphorus recovery from real wastewater, a foil type cathode is recommended to avoid potential losses of small struvite crystals. Also, presence of readily available organic substrates is important to maintain high electric current and establish high local pH conditions near the cathode. Struvite precipitation was relatively slow, requiring 7 days for nearly complete removal (92%) and recovery (96%). Future studies need to focus on shortening the time requirement.

### **Keywords**

Phosphorus recovery; municipal wastewater treatment; struvite; dewatering downstream; microbial electrochemistry; cathode structure



### ***3.1. Introduction***

In conventional wastewater treatment, phosphorus removal is known to be expensive with a large amount of ferric chemical consumption. Biological phosphorus removal also needs large bioreactors to establish anaerobic / aerobic conditions and large pumping capacities to enrich phosphorus accumulating organisms (PAOs) (Daigger et al. 2011; Burton et al. 2013). Another challenge for phosphorus removal in municipal wastewater treatment is the management of downstream wastewater from dewatering processes (i.e., dewatering centrate/filtrate). Such dewatering centrate/filtrate, containing concentrated phosphorus, is often sent back to the mainstream wastewater treatment processes. As a result, phosphorus is continuously recirculated between the mainstream wastewater treatment and sludge treatment systems, making phosphorus removal inefficient in municipal wastewater treatment.

Phosphorus is a valuable resource as it is an essential element in land fertilizers for the agricultural industry and thus closely related to food productivity. Globally mineable phosphorus is owned by only a few countries and thus phosphorus production is expected to decrease by the end of the 21st century (Gilbert 2009), leading to an inevitable drop in food production. Consequently, phosphorus recovery from wastewater has been emphasized in wastewater treatment research so that recovered phosphorus can be used as land fertilizers (Guest et al. 2009; Larsen et al. 2009). While there are a number of methods for phosphorus recovery from nutrient-rich wastewater, such as pyrolysis (Bridle & Pritchard 2004), ion exchange (Liberti et al. 1981), distillation (Udert & Wächter 2012), and algae growth (Cai et al. 2013; El-Shafai et al. 2007), here we focused on the struvite precipitation method ( $\text{MgNH}_4\text{PO}_4 \cdot 6\text{H}_2\text{O}$ ) for efficient phosphorus recovery from dewatering centrate/filtrate in municipal wastewater treatment. Struvite is a nutrient mineral that can be used as a valuable land fertilizer in the agricultural and landscaping industries.

Struvite precipitation requires substantially high pH conditions (Nancharaiah et al. 2016); thus, nutrient recovery as struvite often involves consumption of strong base chemicals in conventional precipitation processes (e.g., NaOH) (El Diwani et al. 2007; Ronteltap et al. 2007; Ryu et al. 2008). Instead of using base chemicals, microbial electrolysis cells (MECs) can be employed to establish high local pH enough to drive struvite precipitation on the cathode as previously demonstrated (Cusick & Logan 2012; Cusick et al. 2014). In MECs, organic substrates are oxidized by exoelectrogenic bacteria at the bioanode and water is reduced to hydrogen gas at the cathode by applying an electric voltage between 0.13 and 1.23 V (Liu et al. 2005; Rozendal & Buisman 2005; Rozendal et al. 2006; Logan et al. 2008; Zhang & Angelidaki 2014). The cathode reaction ( $\text{H}_2\text{O} + 2\text{e}^- \rightarrow \text{H}_2 + 2\text{OH}^-$ ) releases hydroxyl ions, establishing a high local pH near the cathode. The high local pH condition has been utilized in a number of MEC studies to enhance precipitation of various chemicals, including toxic heavy metals (Colantonio & Kim 2016) and struvite crystals (Cusick & Logan 2012; Cusick et al. 2014; Tice & Kim 2014; Qin et al. 2016; Iskander et al. 2015) without adding any base chemicals. Thus, compared to conventional chemical precipitation methods, MECs can produce struvite without using base chemicals. In addition to struvite production, MECs allow energy recovery in the form of hydrogen gas and organic removal in the wastewater.

Since struvite is crystalized on cathode surfaces by high local pH conditions, the cathode configuration plays an important role in efficient struvite production in MECs (Cusick & Logan 2012). While a mesh type cathode was found to be more effective than a plate type cathode in a proof-of-concept study with a relatively small amount of struvite crystals attached on the cathode (Cusick & Logan 2012), a plate-type cathode can be more efficient than the mesh type if an excessive amount of struvite crystals is created and deposited on MEC cathode surfaces. Also,

struvite production in MECs was demonstrated mainly using synthetic solutions (Cusick & Logan 2012; Cusick et al. 2014; Tice & Kim 2014). Thus, potential limitations involved in using real wastewater (e.g., low concentration of readily available organic substrates) were not investigated in the previous studies (Cusick & Logan 2012; Cusick et al. 2014; Tice & Kim 2014; Qin et al. 2016; Iskander et al. 2015). As a result, even though MEC cathodes are proven to drive struvite crystallization from synthetic solutions, there is still a research gap for efficient phosphorus recovery from real wastewater. In this study, we examined dewatering centrate from a local wastewater treatment plant and we also focused on demonstrating complete phosphorus recovery in MECs. To achieve efficient phosphorus recovery, various cathode configurations (mesh vs. foil types; single vs. multiple pieces) were examined in lab-scale MEC experiments for efficient struvite precipitation. In addition, for effective struvite production, high electric current is desired and thus a readily available organic substrate is necessary for MEC operation. Since dewatering centrate is lacking readily available organic substrates, we studied the effect of electric current generation in MECs on the phosphorus recovery. Finally, the time requirement for struvite precipitation was also investigated in this study.

## ***3.2. Methods***

### **3.2.1. Reactor design and construction**

Single-chamber MEC reactors were built with polypropylene blocks and rubber gaskets with a cylindrical inner space (50 mL; 7-cm<sup>2</sup> cross section). The bioanode was a graphite fiber brush (2.5 cm in diameter, 2.0 cm long; Mill-Rose, OH), which was heat treated in a muffle furnace at 450°C for 30 min (Wang et al. 2009). To examine the effect of cathode configuration on phosphorus recovery, stainless steel mesh (SSM) and stainless steel foil (SSF) were used as the cathode in the

MEC. Since struvite is precipitated on cathode surfaces, the amount of cathode surface areas was examined with the SSM cathode (1, 3, or 5 pieces) immersed in the MEC reactor (Figure 3.1A) (6.3-cm<sup>2</sup> cross section; McMaster Carr; 304 stainless steel woven wire cloth; 200 × 200 mesh; 0.053 mm wire diameter) while a single piece of the SSF cathode was located at the end of the MEC reactor (Figure 3.1B) (7.0-cm<sup>2</sup> cross section; Trinity Brand Industries, Inc.; 0.0254 mm thickness). The mesh size (200 × 200) was selected as it produced the highest electric current compared to other commonly available stainless steel mesh sizes (e.g., 50 × 50 or 100 × 100). For the 3- and 5-piece SSM cathode, the distance between the SSM pieces was maintained at ~1 mm using a rubber gasket. The MECs were inclined so that created struvite precipitants can be deposited on the cathode where local pH is maintained high and produced hydrogen gas can be easily removed from the reactor (Figure 3.1). While energy recovery as hydrogen is an important aspect of MEC studies, we focused more on nutrient recovery and wastewater treatability of MECs in this study.

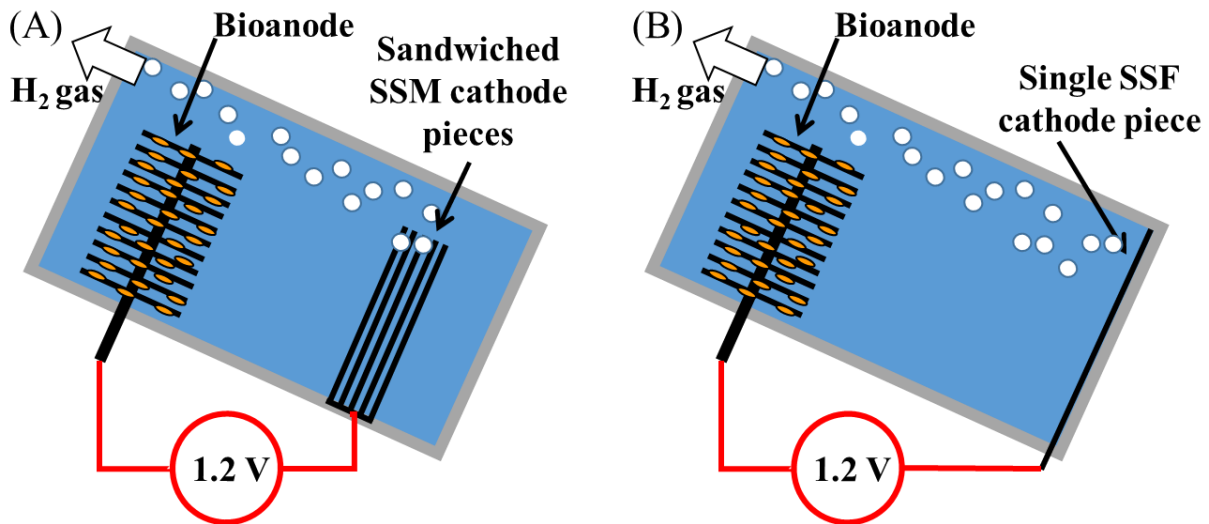


**Figure 3.1 (A) Schematic diagram of MEC constructed with the SSM cathode (5 SSM pieces). (B) Schematic diagram of MEC with the SSF cathode**

### 3.2.2. Reactor start-up and operation

The MECs were inoculated using effluent from an existing MEC. After the start-up operation using acetate as the substrate, the MECs were operated in fed-batch mode using dewatering centrate collected at a local municipal wastewater treatment plant (Additional file 1: Figure S1). Ammonia concentration in the dewatering centrate was  $65.7 \pm 2.8$  mM and phosphate concentration was  $0.43 \pm 0.03$  mM. The ammonia concentration was sufficiently higher than phosphate because struvite precipitation ( $\text{MgNH}_4\text{PO}_4$ ) requires the same molar ratio among magnesium, ammonia and phosphate. The local wastewater treatment plant was operated as conventional activated sludge without biological phosphorus removal; thus, the phosphate concentration in the dewatering centrate could have been higher if biological phosphorus removal had been employed in the mainstream wastewater treatment. Thus, an extra amount of phosphate (1.5, 3.0, or 4.5 mM as  $\text{Na}_2\text{HPO}_4$ ) was added to the dewatering centrate to simulate downstream wastewater from biological phosphorus removal processes. Note that 80% of phosphorus removed from biological phosphorus removal processes is released in anaerobic digestion (American Public Health Association et al. 2012) and the released amount of phosphate can be as high as 2.6 mmol/g-MLSS (mixed liquor suspended solids) (Bond et al. 1999). Thus, we examined various phosphate concentrations in experiments by adding  $\text{Na}_2\text{HPO}_4$  (Table 3.1). For proper struvite precipitation, 2 mM of  $\text{MgCl}_2$  was added in the dewatering centrate for all experimental sets. To investigate the effect of electric current on struvite production,  $\text{NaCH}_3\text{COO}$  was also examined in the MEC operation (Table 3.1).

**Table 3.1 Feed preparation and MEC operation in four experimental sets**

|       |   |
|-------|---|
| Set A | <ul style="list-style-type: none"><li>- 1, 3, 5 SSM cathode pieces</li><li>- No phosphate addition</li><li>- Mg : NH<sub>4</sub> : PO<sub>4</sub> = 2.0 : 66 : 0.43 (mM)</li><li>- No acetate addition</li></ul>  |
| Set B | <ul style="list-style-type: none"><li>- 1, 3, 5 SSM cathode pieces</li><li>- 1.5 mM Na<sub>2</sub>HPO<sub>4</sub> addition</li><li>- Mg : NH<sub>4</sub> : PO<sub>4</sub> = 2.0 : 66 : 1.93 (mM)</li><li>- No acetate addition</li></ul>                |
| Set C | <ul style="list-style-type: none"><li>- Single SSM cathode piece</li><li>- 1.5, 3.0, 4.5 mM Na<sub>2</sub>HPO<sub>4</sub> addition</li><li>- Mg : NH<sub>4</sub> : PO<sub>4</sub> = 2.0 : 66 : 1.93-4.93 (mM)</li><li>- No acetate addition</li></ul>   |
| Set D | <ul style="list-style-type: none"><li>- Single SSF cathode piece</li><li>- 1.5 mM Na<sub>2</sub>HPO<sub>4</sub> addition</li><li>- Mg : NH<sub>4</sub> : PO<sub>4</sub> = 2.0 : 66 : 1.93 (mM)</li><li>- 12.2 mM NaCH<sub>3</sub>COO addition</li></ul> |

Four sets of experiments (Sets A, B, C, and D) were conducted in this study. Sets A and B were designed to investigate the effect of the number of the SSM cathode. In Set C, we studied the effect of various phosphate concentrations assuming biological phosphorus removal processes in the mainstream wastewater treatment. Even though struvite precipitation needs the same molar concentration for Mg<sup>2+</sup>, NH<sub>4</sub><sup>+</sup> and PO<sub>4</sub><sup>3-</sup>, we hypothesized that the kinetics of struvite precipitation can be enhanced by high phosphate concentration. Set D was conducted to improve the struvite recovery using the SSF cathode and high electric current by adding NaCH<sub>3</sub>COO (Table 3.1). The addition of the NaCH<sub>3</sub>COO did not alter the pH of the dewatering centrate, indicating that the dewatering centrate has a sufficient amount of alkalinity.

The applied voltage was 1.2 V using an external power supplier to maximize the electric current in the MEC (GPS-1850D; GW Instek, CA). The electric current was computed by monitoring the voltage crossing an external 10-Ω resistor every 20 min using a digital multimeter

and data acquisition system (Model 2700, Keithley Instruments, OH). All experiments were conducted in an air-conditioned laboratory ( $22.5 \pm 0.2^\circ\text{C}$ ).

### 3.2.3. Experiment measurement

For each fed-batch cycle, the feed and effluent samples were examined for total phosphorus, ammonia and COD (chemical oxygen demand) in accordance with the standard methods (Hach Co.,CO) (American Public Health Association et al. 2012). The experimental samples were also analyzed for pH and conductivity (SevenMulti, Mettler Toledo Group, Switzerland). The conductivity of the dewatering centrate was  $\sim 8.4$  mS/cm and it increased slightly to  $\sim 8.6$  mS/cm during the MEC operation. The feed pH was  $\sim 7.6$  and the effluent pH was  $\sim 8.2$ .

For Sets A and B, the SSM cathode was taken from the MEC reactor after 3 fed-batch cycles and the struvite crystals deposited on the cathode were scraped and dissolved in an acid solution (10 mM HCl) to determine the amount of phosphorus recovered as struvite. The MEC operation over 3 consecutive fed-batch cycles without replacing the cathode allowed investigating the effect of struvite accumulation at cathode surfaces on electric current generation in the MEC. For Sets C and D, the cathode was taken every fed-batch cycle to quantify the precipitated struvite crystals. The phosphorus removal was determined based on the feed and effluent concentration of phosphorus. The amount of phosphorus recovered as struvite was compared with that removed during the MEC operation to determine phosphorus recovery ( $r$ ) as:

$$r = \frac{M_P}{nV(c_{feed} - c_{eff})} \quad (1)$$

$M_P$  is the total moles of phosphorus in struvite precipitants scraped from the cathode,  $n$  is the number of fed-batch cycles (3 for Sets A and B; 1 for Sets C and D),  $V$  is the volume of the MEC

reactor (50 mL),  $c_{feed}$  is the phosphorus concentration in the feed, and  $c_{eff}$  is the phosphorus concentration in the effluent. The precipitated crystals on the cathode were also analyzed in scanning electron microscopy (SEM) and energy dispersive X-ray spectroscopy (EDS) to examine the crystal morphology and identification (JEOL JSM-6610LV, Japan). The EDS analysis results confirmed that the precipitants on the MEC cathode are struvite (Additional file 2: Figure S2).

The Coulombic efficiency (CE) was determined by dividing the amount of electrons measured in electric current by the amount of electrons that can be yielded from substrate removal as (Logan et al. 2008):

$$CE = \frac{8 \int I dt}{FV\Delta COD} \quad (2)$$

$I$  is the electric current,  $F$  is the Faraday constant, and  $\Delta COD$  is the COD removal over a fed-batch cycle. The electric energy requirement ( $W_E$ ) was calculated using (Logan et al. 2008):

$$W_E = \int (IE_{ap} - I^2 R_{ext}) dt \quad (3)$$

$E_{ap}$  is the applied voltage (1.2 V) and  $R_{ext}$  is the external resistor (10  $\Omega$ ).

### ***3.4. Results and discussion***

#### **3.4.1. SSM cathode for struvite production**

The phosphorus removal of each fed-batch cycle was consistently high (69-85%) with the SSM cathode in Sets A and B (Table 3.2). No clear correlation was found between the phosphorus removal and number of SSM pieces, indicating that the total surface area of the SSM cathode did not limit the phosphorus removal by struvite precipitation. In Sets A and B, struvite precipitants



were obtained on the cathode after 3 fed-batch cycles and the majority of the precipitants were found on the SSM piece located close to the bioanode.

**Table 3.2 Phosphorus removal and recovery (n = 3; mean ± standard error)**

| Experiment | Number of SSM cathode | Phosphorus in feed | Phosphorus in effluent | Removal     | Recovery as struvite |
|------------|-----------------------|--------------------|------------------------|-------------|----------------------|
| Set A      | 1 piece               | 0.43 ± 0.03 mM     | 0.13 ± 0.01 mM         | 69.7 ± 0.8% | 54.0%                |
|            | 3 pieces              |                    | 0.13 ± 0.01 mM         | 70.6 ± 0.5% | 55.6%                |
|            | 5 pieces              |                    | 0.13 ± 0.01 mM         | 69.3 ± 0.5% | 68.2%                |
| Set B      | 1 piece               | 1.28 ± 0.09 mM     | 0.23 ± 0.01 mM         | 82.4 ± 0.2% | 10.3%                |
|            | 3 pieces              |                    | 0.26 ± 0.04 mM         | 80.0 ± 2.8% | 15.7%                |
|            | 5 pieces              |                    | 0.20 ± 0.03 mM         | 84.7 ± 1.1% | 26.8%                |
| Set C      | 1 piece               | 1.36 mM            | 0.18 mM                | 87.0%       | 6.8%                 |
|            |                       | 2.63 mM            | 0.37 mM                | 86.0%       | 6.1%                 |
|            |                       | 3.26 mM            | 0.70 mM                | 78.6%       | 22.5%                |

By comparing the amount of phosphorus in the deposited struvite crystals with that removed during the MEC operation (Eq. 1), the phosphorus recovery in Set B was relatively low at 10-27% than that in Set A (54-68%). This drop in the phosphorus recovery with the increased phosphate concentration in Set B indicates that the SSM cathode has a limited capacity to hold produced struvite crystals. In addition, the phosphorus recovery showed increasing trends for both Sets A and B with the increasing number of cathode pieces (Table 3.2). The increased surface area of the SSM cathode did not affect the phosphorus removal but improved the phosphorus recovery. However, the phosphorus recovery was below 27% especially when additional phosphate was provided in the dewatering centrate.

Three different phosphate concentrations (1.36, 2.63, and 3.26 mM) were examined in the experimental Set C to simulate downstream wastewater from enhanced biological phosphorus removal processes (Bond et al. 1999; Mavinic et al. 1998). The phosphorus removal efficiency was maintained high at 78-87% with only a single SSM piece as the cathode (Table 3.2). Thus, the

single-piece SSM cathode was sufficient to remove phosphate for the examined concentrations. However, the phosphorus recovery as struvite crystals on the cathode was insufficient and varying a wide range between 6 and 20% (Table 3.2).

The difference between the high removal and low recovery can be explained by relatively small struvite crystals on the cathode. The SEM images showed that the majority of struvite crystals are smaller than 10  $\mu\text{m}$  (Additional file 3: Figure S3). As a result, struvite crystals were easily lost through the open mesh spaces when the MEC reactors were disassembled to collect precipitated struvite crystals. Note that the SSM cathode had much larger open spaces between woven wires (80  $\mu\text{m}$   $\times$  80  $\mu\text{m}$ ) than produced struvite crystals (a few to tens of micrometers). Thus, the SSM cathode was effective to drive struvite precipitation as previously proven (Cusick & Logan 2012); however, it was not ideal for holding precipitated crystals especially when the cathode was practically covered by struvite precipitants (Additional file 4: Figure S4).

### **3.4.2. Electric current and COD removal**

There was no clear correlation between the electric current and number of SSM cathode pieces (Figure 3.2A), indicating that the electric current generation was not limited by the cathode. The electric current density was mostly below 0.02  $\text{A}/\text{m}^2$  (Figure 2). As a result, the COD removal was relatively low, varying over a wide range from 15 to 39% (Table 3.3). The limited COD removal as well as the low electric current can be explained by the limited amounts of readily available organic substrates in the dewatering centrate for exoelectrogens. Note that concentration of acetic acid or other volatile fatty acids is relatively low in sludge treated in healthy anaerobic digesters (Rittmann & McCarty 2012; Asztalos & Kim 2015; Yang et al. 2015). Since the MEC operation was limited by low readily available organic substrate concentration, the increasing cathode

surface area did not effectively increase the electric current with 1, 3 and 5 cathode pieces (Figure 3.2A). Thus, the relatively high COD in the dewatering centrate (487 to 800 mg COD/L) was not favorably utilized by exoelectrogenic microorganisms at the bioanode. As a result, the Coulombic efficiency (CE) was relatively low and varied widely from 3 to 86% (Table 3.3). In addition to the large open area of SSM, the low electric current was also considered to result in a limited struvite recovery (Table 3.2) because a sufficiently high local pH near the cathode was not established due to slow creation of hydroxyl ions (i.e., slow consumption of proton ions).

**Table 3.3 COD removal and Coulombic efficiency (n = 3; mean ± standard error)**

| Experiment | Number of SSM cathode | COD in feed   | COD in effluent | COD Removal  | Coulombic Efficiency |
|------------|-----------------------|---------------|-----------------|--------------|----------------------|
| Set A      | 1 piece               | 600 ± 21 mg/L | 437 ± 64 mg/L   | 26.9 ± 11.1% | 86.3 ± 64.6%         |
|            | 3 pieces              |               | 367 ± 12 mg/L   | 38.6 ± 4.2%  | 29.9 ± 6.5%          |
|            | 5 pieces              |               | 457 ± 30 mg/L   | 24.0 ± 3.1%  | 54.2 ± 17.4%         |
| Set B      | 1 piece               | 487 ± 35 mg/L | 407 ± 22 mg/L   | 16.2 ± 2.3%  | 10.4 ± 1.0%          |
|            | 3 pieces              |               | 397 ± 27 mg/L   | 18.4 ± 1.3%  | 26.7 ± 15.1%         |
|            | 5 pieces              |               | 367 ± 43 mg/L   | 24.5 ± 7.7%  | 18.7 ± 15.6%         |
| Set C      | 1 piece               | 730 mg/L      | 460 mg/L        | 37.0%        | 2.5%                 |
|            |                       | 630 mg/L      | 480 mg/L        | 23.8%        | 5.5%                 |
|            |                       | 800 mg/L      | 680 mg/L        | 15.0%        | 9.7%                 |

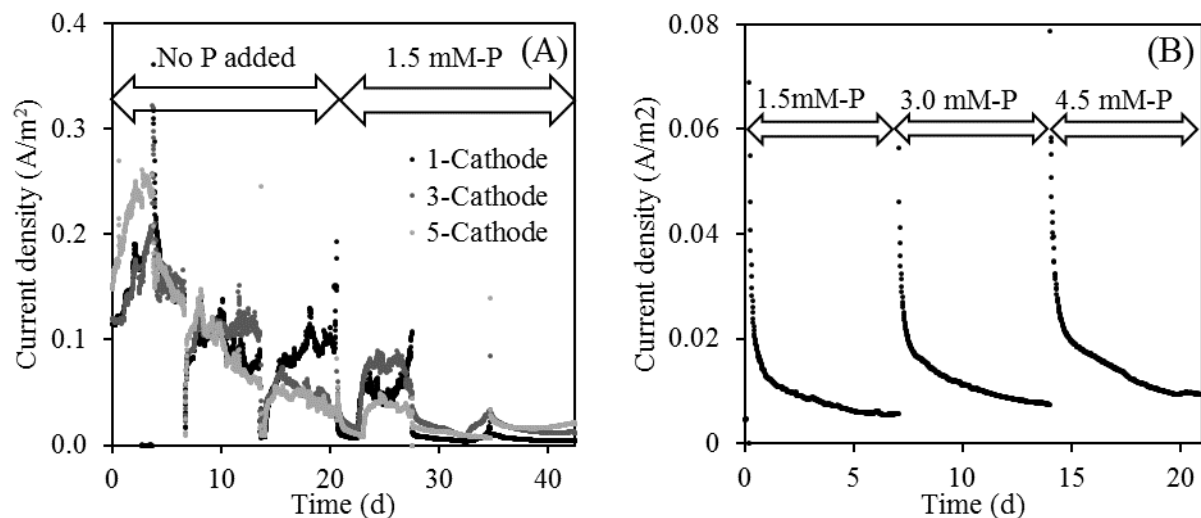


**Figure 3.2 Electric current generation in MECs with the SSM cathode: (A) effect of the number SSM pieces in Sets A and B; (B) effect of phosphate concentration in Set C**

### 3.4.3. Enhanced struvite recovery with SSF and high electric current

To improve the struvite recovery, the SSF cathode was used in the MEC and high electric current was induced by adding acetate in the dewatering centrate in Set D. The phosphorus removal was 53% in only one day and it increased to 92% in 7 days (Figure 3.3). The phosphorus recovery substantially improved from 18% to 96% with the increased MEC operation (Figure 3.3). This result indicates that high electric current and a foil type cathode are necessary to maintain high phosphorus recovery. The high electric current density helped to maintain high local pH near the cathode with a high rate of the hydroxyl ion release from water electrolysis (Figure 3.4). Also, the phosphorus recovery as the cathode precipitant was usually lower than the removal (Figure 3.3). The phosphorus uptake by microorganisms can potentially explain the discrepancy between the removal and recovery; however, a more systematic approach is necessary to quantify the contribution by microbial uptake in future studies.

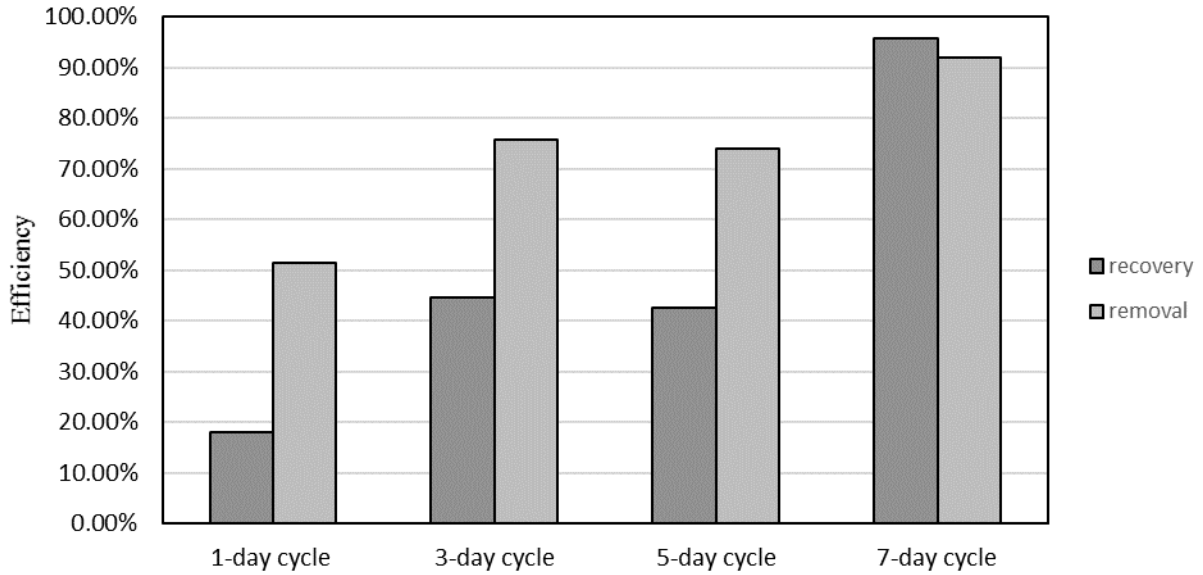


**Figure 3.3 Phosphorus removal and recovery with the SSF cathode (Set D)**

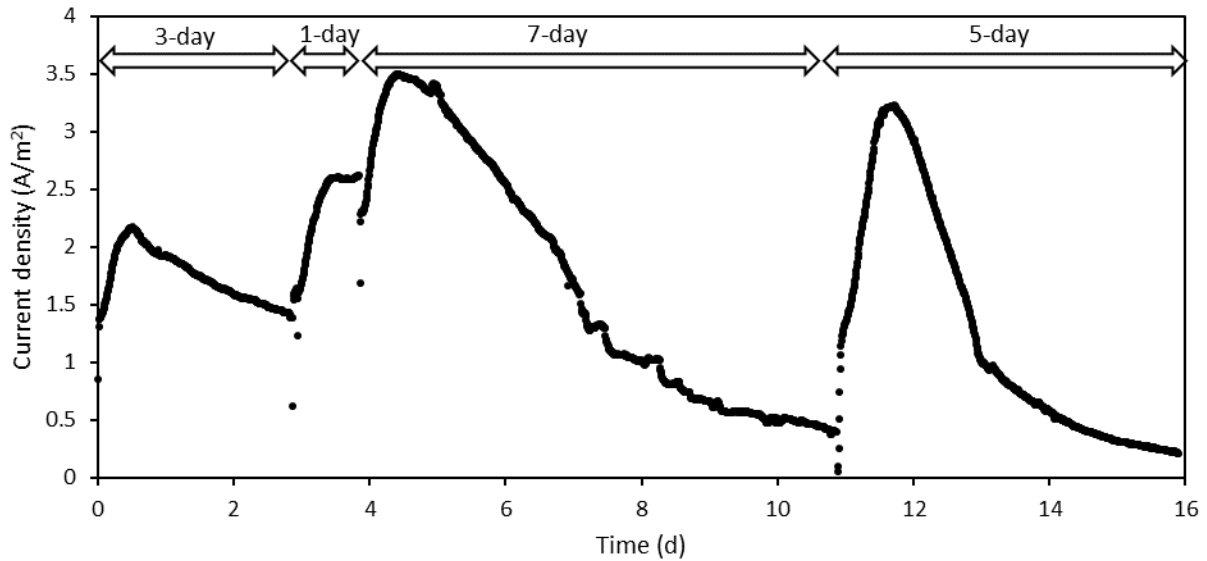


**Figure 3.4 Electric current generation in during the MEC operation with the SSF cathode (Set D)**

In the previous studies, a mesh type cathode worked better for phosphorus removal (40% removal) compared to a foil type cathode (26% removal) (Cusick & Logan 2012). However, when the amount of phosphorus recovered is substantially large, the SSF cathode resulted in high removal and recovery in this study. Note that the SSF cathode was fully covered with struvite salts in this study (Additional file 5: Figure S5). In a separate experiment (not shown), we also operated the MEC with SSM cathode and acetate; however, the phosphorus recovery was not as high as that with SSF and acetate, indicating that the cathode structure is more important than the presence of a readily available organic substrate.

#### **3.4.4. Energy requirement for struvite production**

The electric energy consumption was 843 J ( $2.34 \times 10^{-4}$  kWh) for the operation of the MEC with the SSF cathode over 7 days (Eq. 3). Based on this energy consumption, 4.95 MJ (13.8 kWh) is estimated to be necessary to produce 1 kg of struvite from dewatering centrate. Similarly, the energy requirement was 1.09 MJ (0.30 kWh) per 1 kg struvite production without adding acetate in Set C. Note that the energy recovered as H<sub>2</sub> gas was not considered in the energy estimation; thus, the net energy requirement will be substantially smaller as previously discussed (Cusick & Logan 2012). Considering the relatively low energy requirement and enhanced phosphorus recovery, MECs have strong potential for struvite production from nutrient-rich wastewater streams.

### ***3.5. Conclusions***

The SSM and SSF cathodes were examined in lab-scale MECs to improve the phosphorus recovery from dewatering centrate. The SSM cathode was effective in removing phosphorus via struvite precipitation but the phosphorus recovery was insufficient (maximum 68%) because the open space between woven wires ( $80\ \mu\text{m} \times 80\ \mu\text{m}$ ) was much larger than the size of struvite crystals (a few to tens of micrometers). As a result, the phosphorus recovery was not sufficiently improved by increasing the surface area of the cathode up to 5 SSM pieces.

The dewatering centrate from conventional anaerobic digesters contained a small amount of readily available organic substrates for exoelectrogenic bacteria at the bioanode. As a result, the electric current was substantially low in the MEC reactors, resulting in slow water electrolysis at the cathode. Consequently, the local pH near the cathode was not sufficiently high, leading to the limited recovery of struvite from the dewatering centrate. Thus, readily available organic substrates need to be provided in MECs for efficient recovery of phosphorus as struvite.

The SSF cathode was then examined to minimize potential losses of small struvite crystals and acetate was added in the MEC operation as a readily available organic substrate. The high electric current density ( $>2\ \text{A}/\text{m}^2$  for peak currents) and foil type cathode resulted in successful struvite production from dewatering centrate with 92% removal and 96% recovery. The phosphorus removal and recovery efficiencies increased with the increasing fed-batch cycle period. A retention time of 7 days was necessary to achieve complete removal and recovery of phosphorus in the SSF MEC. MECs have potential for struvite production in municipal wastewater treatment plants with a relatively small electric energy requirement: 13.8 kWh per kg struvite production with acetate and 0.30 kWh without acetate. While we demonstrated high energy efficiency and enhanced phosphorus recovery from a real wastewater stream, the purity of the struvite precipitants

was not examined in this study. Various MEC operating conditions need to be investigated for their effects on the purity of struvite crystals in future studies.



## 4. Bioanode sensor for rapid organic detection in water systems

### *Abstract*

Bioanode sensors utilizing exoelectrogenic bacteria can be used for real-time and in-situ assessment of water quality. The main challenges for practical applications of bioanode sensors in water quality assessment include the narrow detection range, long analysis time, and hysteresis effect. To overcome these limitations, a new operation method was proposed and examined using microbial electrolysis cell-based bioanode sensors. The new operating method consists of Normal Operation (0.6 V application), Reset Step (1.8 V application for 1 min), and Test Step (1.2 V application for 2 min). The Reset Step operation eliminated potential hysteresis effects and thus resulted in accurate correlations between soluble COD (chemical oxygen demand) and electric current with consistent  $R^2$  values of 99% in triplicated sensor experiments. The high voltage application (1.2 V) during Test Step enhanced the sensor accuracy and extended the detection range up to 130 mg-COD/L. The combination of Reset Step and Test Step was proven to allow reliable sensor applications of bioelectrochemical systems. Even with the greatly improved sensor accuracy, the correlation between soluble COD and electric current varied substantially over 2 days, requiring frequent sensor calibration. Overall, the proposed sensor operation method allowed rapid and reliable measurement of biodegradable organics using exoelectrogenic bacteria.

### **Keywords**

Bioanode sensor; microbial electrolysis cells; microbial electrochemistry; organic detection; real-time monitoring

#### **4.1. Introduction**

Bioelectrochemical systems are an emerging technology for sustainable wastewater treatment and resources recovery (Cusick et al. 2014; Cusick & Logan 2012; Tice & Kim 2014; Yuan et al. 2016; Ichihashi & Hirooka 2012; Hirooka & Ichihashi 2013). Another potential application of bioelectrochemical systems is the bioanode sensors for real-time and in-situ detection and monitoring of biodegradable organics in engineered systems as well as in natural water systems (Kumlanghan et al. 2007; Zhang & Angelidaki 2011; Jin et al. 2016; Yang et al. 2016; Di Lorenzo et al. 2009; Chang et al. 2004; Quek et al. 2014; Karube et al. 1977). Quantification of biodegradable organics provides essential information for water quality assessment. The amount of organics is measured as biochemical oxygen demand (BOD) and chemical oxygen demand (COD). The BOD measurement takes 5 days and is affected by various factors, such as seed bacteria, initial dissolved oxygen levels, and dilution ratios. COD can be measured quickly in 2 hours; however, the strong oxidizing capacity of dichromate often overestimates biodegradable organics in samples. In addition, BOD and COD analyses require various laboratory instruments, such as incubators, dissolved oxygen meters, spectrophotometers, and digesters. Thus, the conventional analytical methods can hardly be used as real-time and in-situ sensor tools in monitoring essential water quality parameters.

Bioanode sensors are a new analytical technology to utilize exoelectrogenic bacteria (*Geobacter* and *Shewanella* spp.) that oxidize biodegradable organics and generate measurable electric signals by transferring electrons to the bioanode (Logan et al. 2006; Logan et al. 2008). Thus, the bioanode sensors can be used as real-time and in-situ monitoring tools for biodegradable organics (Kumlanghan et al. 2007; Zhang & Angelidaki 2011; Jin et al. 2016; Yang et al. 2016; Di Lorenzo et al. 2009; Chang et al. 2004; Quek et al. 2014; Karube et al. 1977; Sakaguchi et al.

2003; Sakaguchi et al. 2007), volatile fatty acids (Jin et al. 2016; Kaur et al. 2013; Kaur et al. 2014; Bond et al. 1999; Cerrillo et al. 2016), dissolved oxygen (Zhang & Angelidaki 2012), and metal toxicity (Modin et al. 2012). Bioanode sensors are usually operated as microbial fuel cells (MFCs) (Stein et al. 2012; Kumlanghan et al. 2007; Di Lorenzo et al. 2009; Zhang & Angelidaki 2011; Chang et al. 2004; Kaur et al. 2014; Baeza et al. 2016; Zhang & Angelidaki 2012) or microbial electrolysis cells (MECs) (Quek et al. 2014; Jin et al. 2016). In MFCs, the cathode reaction (reduction of oxygen) is coupled with the bioanode reaction and the electrode reactions are driven spontaneously, creating electric power (Logan et al. 2006). Thus, MFC-based bioanode sensors are suitable for remote monitoring of organic amounts in natural waters and sediments. On the other hand, MEC-based bioanode sensors are operated with the cathode for hydrogen evolution reaction. Even though MEC-based sensors requires a small applied voltage ( $E_{ap} > 0.2$  V) (Logan et al. 2008), the cathode can be immersed in water without a continuous supply of oxygen. In addition, MEC-based bioanode sensors can monitor biodegradable organics over a wide concentration range (Modin et al. 2012). Thus, MEC-based sensors are considered to be more suitable for water quality monitoring in engineered systems, such as wastewater treatment processes. Recent studies have demonstrated that MEC-based bioanode sensors can be used to monitor volatile fatty acid levels in anaerobic digestion (Jin et al. 2016). Even with these successful demonstrations, bioanode sensors are rarely used as practical monitoring tools in full-scale wastewater treatment plants.

A key challenge for bioanode sensor applications is their inconsistent current generation results depending on the history of bioanode operation. For instance, when the bioanode sensor is exposed to high organic conditions, the exoelectrogenic bacteria can generate relatively high electric current even at low organic concentrations by endogenous decay. The main objective of

this study was to propose an MEC operation sequence for accurate and rapid detection of biodegradable organics using bioanode sensors. In the MEC operation sequence development, we focused on demonstrating the elimination of the hysteresis effect on the bioanode signal by introducing a very high voltage application ( $E_{ap} = 1.8$  V) for a short period of time (1 min). We examined how the high voltage application can shorten the time requirement for steady-state electric current generation in the bioanode sensor. Another aspect of this study was to investigate how applied voltages affect bioanode sensor performance. In this investigation, we hypothesized that electric current generation by exoelectrogenic bacteria is more significantly affected by the substrate concentration at high voltage conditions (e.g., 1.2 V). As a result, the electric sensor signals can be more reliably correlated with the organic concentration. Finally, changes in bioanode sensor performance with time were also monitored to identify potential challenges for microbial electrochemistry applications for real-time and in-situ detection of biodegradable organics in various water systems.

## **4.2. Methods**

### **4.2.1. Sensor construction and start-up**

Three lab-scale bioanode sensors were prepared in single-chamber MEC reactors. Each MEC was assembled with polypropylene blocks with a cylindrical inner space (50 mL; 7-cm<sup>2</sup> cross section). A surfactant-pretreated graphite fiber brush (Mill-Rose, USA) was used as the bioanode (Guo et al. 2014). The size of the graphite brush was reduced by removing ~80% of the graphite fibers. This reduction of the bioanode size was necessary so that electric current in the sensor can be limited at the bioanode. The cathode was woven mesh stainless steel (6.3-cm<sup>2</sup> cross section; McMaster Carr; 200 × 200 mesh). The cathode was pretreated by electrodepositing platinum at

1.5 V for 5 hours in a platinum chloride solution (0.9 mM Na<sub>2</sub>PtCl<sub>6</sub>; 0.5 mM H<sub>2</sub>SO<sub>4</sub>) (Hu et al. 2009; Hrapovic et al. 2010). The bioanode sensors were inoculated with effluent from existing MECs and operated as MECs at an applied voltage ( $E_{ap}$ ) of 0.6 V until the bioanode generated stable electric current.

#### **4.2.2. Sensor operation**

The bioanode sensor was fed with a solution containing 2.56 mM sodium acetate (120 mg-COD/L), 1.145 g/L Na<sub>2</sub>HPO<sub>4</sub>, 0.613 g/L NaH<sub>2</sub>PO<sub>4</sub>-H<sub>2</sub>O 16.13mM Na<sub>2</sub>HPO<sub>4</sub>, 8.88 mM NaH<sub>2</sub>PO<sub>4</sub>, and trace vitamins and minerals (Cheng et al. 2009). A multi-channel potentiostat (MGP-2, BioLogic, France) was used to apply various voltages and monitor electric current in the bioanode sensors every second. Two sets of sensor experiments were conducted simultaneously using the 3 bioanode sensors. In Set 1, the bioanode sensors were operated at  $E_{ap}$  of 0.6 V for 58 min (Normal operation). After Normal operation, the applied voltage was 1.2 V for 2 min (Test Step). In Set 2, Normal operation was 57 min (one minute shorter than that in Set 1) and followed by  $E_{ap}$  of 1.8 V for 1 min (Reset Step) and then 1.2 V for another 2 min (Test Step) (Figure 4.1). At the end of the 2-min Test Step, 4.5 mL of sample was taken from the sensor reactor for COD analysis and the sequence of Normal operation, Reset Step, and Test Step was repeated (Figure 4.1).

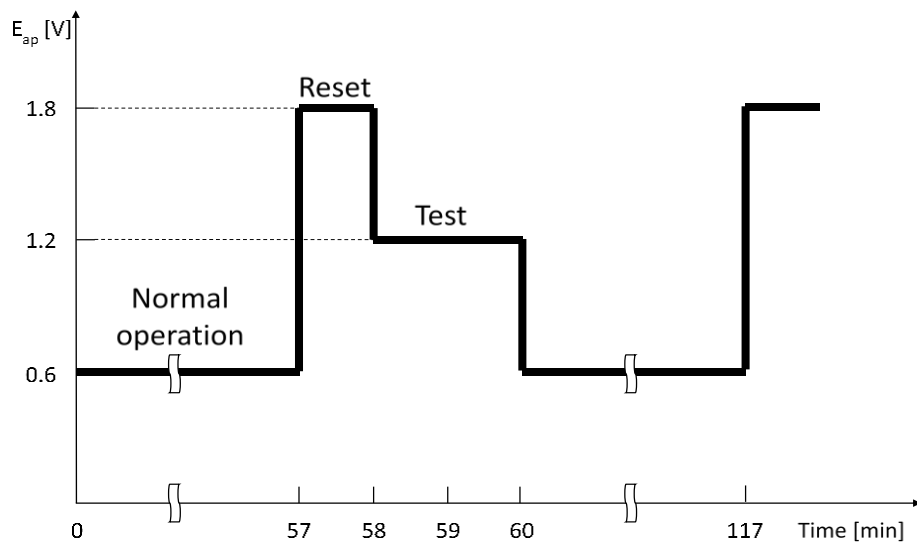


**Figure 4.1** Sequence of applied voltage in Set 2

#### 4.2.3. Experimental measurement

The collected sample was filtered (pore size 0.45  $\mu\text{m}$ , polyethersulfone membrane, VWR International, Canada) and analyzed for chemical oxygen demand (COD) according to the standard methods (Hach Co., USA). Note the COD analysis was conducted as duplicates for every sample. The conductivity and pH of the feed solution were stable at  $\sim 4.02$  mS/cm and  $\sim 7.2$  (SevenMulti, Mettler Toledo Group, Switzerland). All the sensor experiments were conducted in an air-conditioned laboratory and the temperature was constant at  $22.1 \pm 0.7^\circ\text{C}$ .

### 4.3. Results and discussions

#### 4.3.1. Bioanode sensor performance without Reset or Test Steps

Relatively weak positive relationships ( $R^2 = 64\text{-}94\%$ ) were observed between the sCOD (soluble COD) and electric current generation, and an accurate linear relationship could not be established

when the electric current was collected at the end of *Normal operation* (i.e., no Reset or Test Step) (Figure 4.2). The electric current in the three sensors was saturated and became stationary when the sCOD concentration was approximately 75 mg/L or higher. This observation indicates that the upper detection limit was ~75 mg/L as sCOD for the bioanode sensors. This finding is consistent with previous reports where the half saturation constant for exoelectrogenic bacteria is relatively small and can be as small as 7.02 mg-COD/L (Torres et al. 2007; Pinto et al. 2010). As a result, the electric current became constant and no noticeable increases were observed when sCOD was greater than 75 mg/L. The relatively low detection limit implies that bioanode sensors are more suitable for the detection of organics in natural water systems or municipal wastewater treatment processes, rather than treatment systems for high strength wastewater.

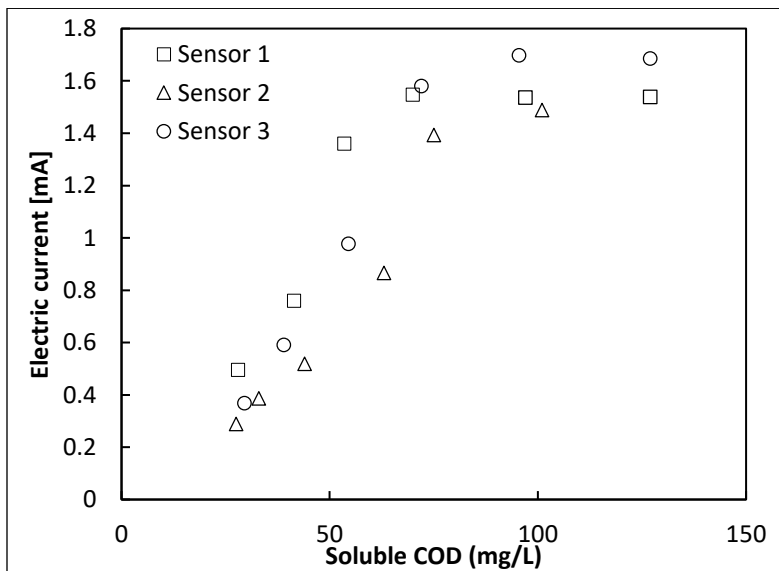


**Figure 4.2** Correlation between sCOD and electric current at the end the Normal operation (No Reset Step; No Test Step) in Set 1

#### 4.3.2. Effects of $E_{ap}$ on sensor reliability

A clear linear relationship ( $R^2 = 95-98\%$ ) between the sCOD and electric current generation was obtained at the end of *Test* Step ( $E_{ap} = 1.2$  V) in Set 1 without the *Reset* Step (Figure 4.3). Compared to the results at  $E_{ap}$  of 0.6 V (Figure 4.2), the higher  $E_{ap}$  of 1.2 V substantially enhanced the electric signal sensitivity to sCOD. In addition, the linear correlation was maintained for the examined sCOD concentration; thus, the upper detection limit of the sensors was increased above 125 mg-sCOD/L for the increase with the 1.2-V Test Step. Even though this finding is not consistent with a recent report (Jin et al. 2016), it is reasonable to assume that bioanode bacteria have a greater exoelectrogenic capacity at higher applied voltage conditions. At a higher voltage application condition, in addition, the effect of uncertainty factors other than substrate concentration becomes negligible on the electric current generation. As a result, the  $R^2$  value has greatly improved with the 1.2 V Test Step (Figure 4.3). Note that the time requirement for Test Step (2 min) is relatively shorter than that proposed in previous studies (Quek et al. 2014; Jin et al. 2016).



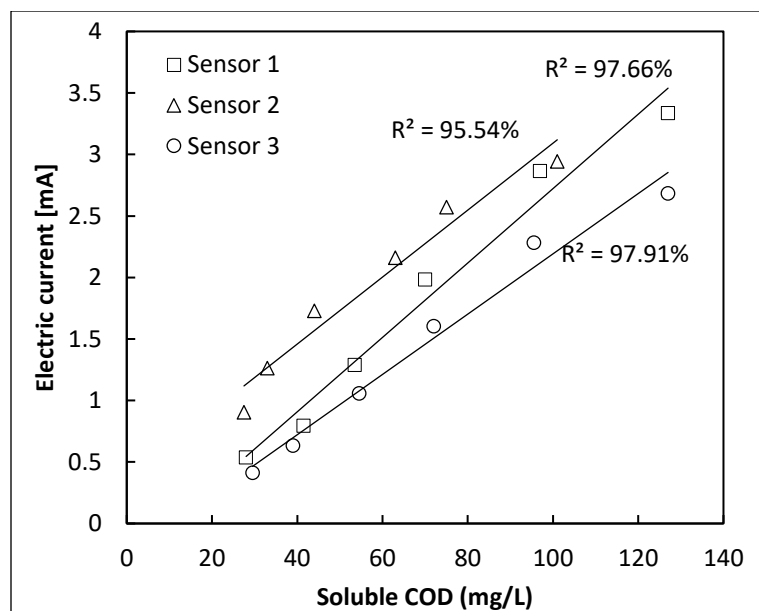


**Figure 4.3** Correlations between sCOD and electric current at the end of Test Step (No Reset Step) in Set 1

#### 4.3.4. Role of Reset Step

Reset Step ( $E_{ap}$  of 1.8 V for 1 min) further improved the correlation between the sCOD concentration and electric current generation as the  $R^2$  value was consistently 99% among the triplicated sensor experiment (Figure 4.4). The high  $R^2$  values verified the strong potential of bioanode sensors for organic detection and quantification above 100 mg-sCOD/L. It should be emphasized that the time requirement of Reset Step was only 1 min, allowing rapid and reliable monitoring of water quality using the bioanode sensor.

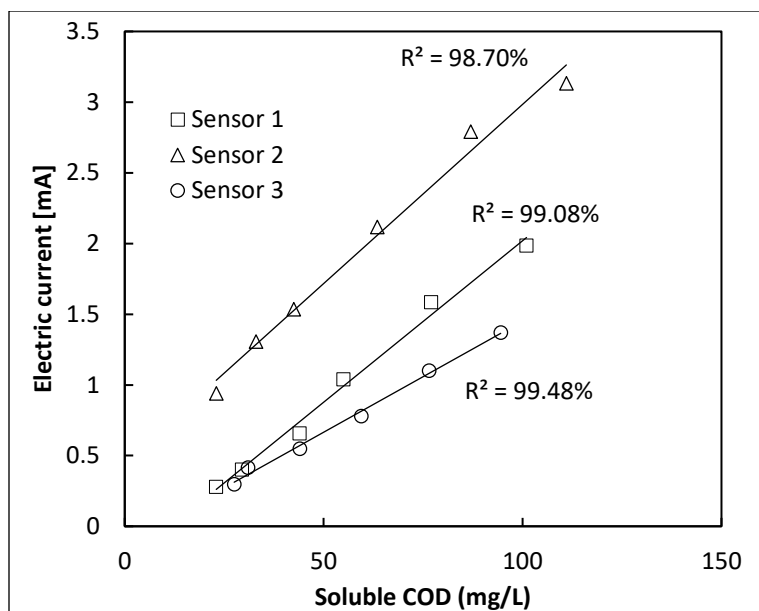


**Figure 4.4** Correlations between sCOD concentration and electric current with Reset Step in Set 2

The sensor experimental results with Reset Step were summarized into three sensor equations for the prediction of sCOD concentration using electric current (I) from the bioanode sensors (Table 4.1). Using the equations, the sCOD concentration can be determined using the electric current from the bioanode sensor.

**Table 4.1** Sensor calibration equations obtained by linear regression from experiments with Reset Step in Set 2

|          |                         |                 |
|----------|-------------------------|-----------------|
| Sensor 1 | $sCOD = 43.38I + 11.97$ | $R^2 = 99.08\%$ |
| Sensor 2 | $sCOD = 38.95I - 16.74$ | $R^2 = 98.70\%$ |
| Sensor 3 | $sCOD = 63.32I + 7.89$  | $R^2 = 99.48\%$ |

The role of *Reset Step* was found to shorten the time requirement for stable electric current generation in the bioanode sensor (Figure 4.5). In Set 1, the sensor was operated without Reset

Step while Reset step was assigned just before Test Step in Set 2. Without Reset Step, the electric current continuously decreased over the 2-min Test Step (dashed lines in Figure 4.5). With Reset Step, however, the electric current generation reached a constant value in less than one minute (solid lines in Figure 4.5). This result demonstrates that Reset Step eliminates potential hysteresis effects of the bioanode bacteria so that bioanode sensors can generate steady-state electric current signals in one minute. Rapid steady-state current generation with Reset Step explains the excellent R2 values in the bioanode sensor experiments (Figure 4.4). In previous studies, reliable sensor performance was often achieved by having a long starvation period up to 10hr (Chang et al. 2004; Jin et al. 2016; Quek et al. 2014) or by implementing specific electrode operation (Kaur et al. 2014). As a result, it took a relatively long time to obtain sensor signals for reliable determination of organic concentration. However, the proposed *Reset Step* method was proven to allow a rapid organic analysis in 3 min (1-min of Reset Step and 2-min of Test Step).

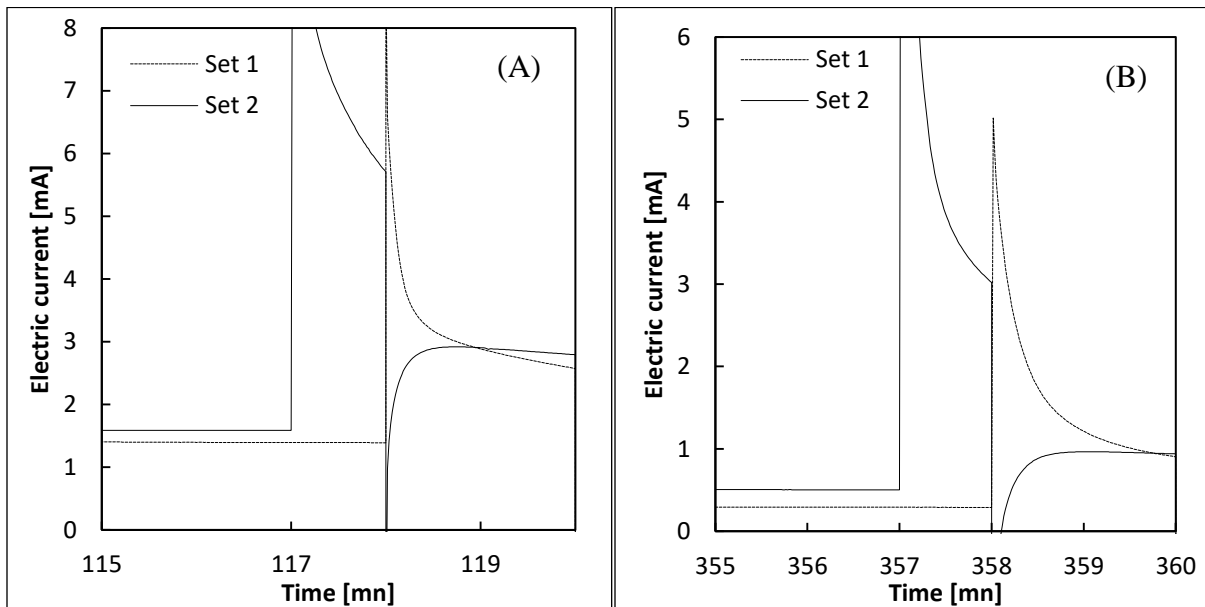


**Figure 4.5** Electric current variation in Sensor 2 during Test Step with and without Reset Step at (A) relatively high sCOD concentration and (B) low sCOD concentration

### 4.3.5. Challenges in bioanode sensor applications

Even though the proposed Reset Step method was proven to generate accurate bioanode sensor results with consistently high R2 values (Figure 4.4), there still remain challenges in utilizing the bioanode as a reliable sensor. In Table 4.1, the sensor calibration equations were not consistent among the 3 bioanode sensors. This inconsistency indicates that bioanode sensors must be calibrated individually. That is, a calibration equation for a bioanode sensor cannot be used for other bioanode sensors. In addition, we found that the calibration equation for the same bioanode sensor varies with time. For instance, the slope of the linear relationship between sCOD and electric current changed substantially in 2 days for Sensor 1 (Figure 4.6). This finding indicates that bioanode sensors must be calibrated frequently and the future research on bioanode sensor applications should focus on demonstrating consistent sensor performance over an extended time period.

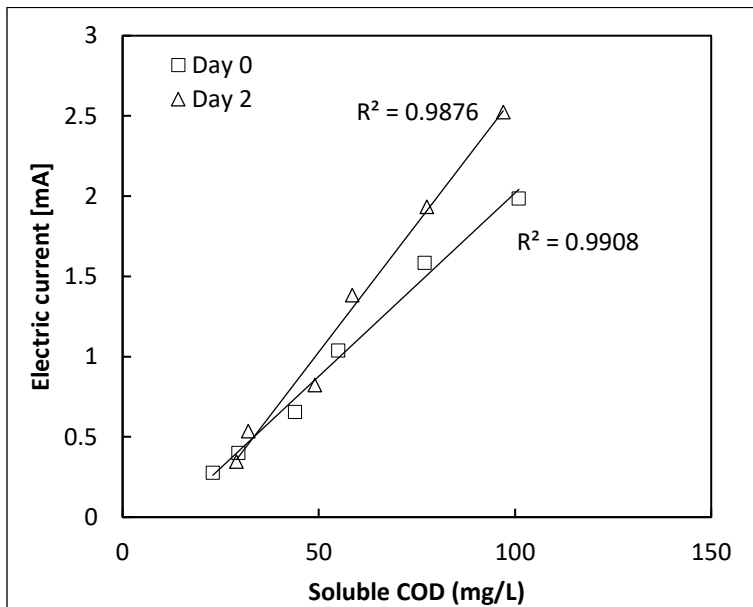


*Figure 4.6 Changes in the sensor correlation with time in Sensor 1 with Rest Step*

#### ***4.4. Conclusions***

This study examined new sensor operation sequences to eliminate the hysteresis effects of bioanode sensors. Accurate linear correlations were established between the electric current and sCOD concentration ranging up to 130 mg/L. The sensor accuracy was greatly improved to the consistent  $R^2$  value of 99% in the triplicate experiment by implementing *Reset* Step. The high voltage application ( $E_{ap} = 1.8$  V) for 1 min during *Reset* Step was found to help exoelectrogenic bacteria generate steady-state electric current during *Test* Step. The bioanode sensors were found to be more accurate for high voltage applications. At the end of *Normal Operation* ( $E_{ap}$  of 0.6 V), the electric current was not clearly correlated with the sCOD concentration. However, the 1.2 V application during *Test* Step resulted in more accurate correlations between the electric current and sCOD. In addition, the higher voltage application was found to increase the upper detection limit from 75 to 130 mg-COD/L. Based on the COD detection range, bioanode sensors are considered to be suitable for monitoring biodegradable organics in natural water systems or municipal wastewater treatment processes. Moreover, the proposed method with *Reset* and *Test* Steps showed rapid monitoring of biodegradable organics in 3 min. Even if accurate correlations between sCOD and electric current can be established using the proposed method, the correlations varied substantially with time, requiring daily calibration for reliable sensor applications. We recommend that future studies focus on resolving this limiting factor for practical bioanode sensor applications in natural and engineered water systems.

## 5. Conclusions

### *5.1 Phosphorus recovery using microbial electrolysis cells*

The lab-scale microbial electrolysis cells (MECs) were examined for increasing phosphorus recovery from dewatering centrate. The stainless steel mesh (SSM) cathode reactors demonstrated inefficient removal and recovery because the open space between woven wires ( $80\ \mu\text{m} \times 80\ \mu\text{m}$ ) on the SSM cathode was too large to hold struvite crystals which were a few to tens of micrometers. On the other hand, the dewatering centrate contained limited readily biodegradable organic substrate which caused low electric current density in the reactors. Thus, the local pH near the cathode was not high enough to promote struvite precipitation.

The SSM cathodes were then replaced by the stainless steel foil (SSF) cathodes to minimize potential losses of struvite crystals. Also, sodium acetate was added to the feed solution as supplementary readily biodegradable organic substrate. As a result, 92% removal and 96% recovery were achieved in the SSF MEC. Moreover, the energy requirement of using MEC for phosphorus recovery was estimated as 13.8 kWh per kg struvite production which was significantly lower than that of using conventional methods.

### *5.2 Organic detection using microbial electrolysis cells*

A MEC-based bioanode sensor was investigated with new operation sequences to eliminate the hysteresis effect. Two sets of experiments were conducted and both produced accurate linear correlations. In particular, Set 2 with both *Reset* step and *Test* step further improved determination coefficients from 97% to 99%. As a result, the proposed operation sequences achieved rapid organic detection in 3 min. Moreover, it was shown that *Reset* step could help the electric current

during *Test* step reach steady state within 1 min. Also, the upper detection limit was found to increase from 75 to 130 mg-COD/L as the applied voltage was increased. The observed detection range made the bioanode sensors feasible for monitoring biodegradable organics in natural or engineered water systems. Even if accurate correlations between sCOD and electric current can be established using the proposed method, a daily calibration is recommended due to continuous variation of microbial activity with time.

### **5.3 Future work**

This thesis has demonstrated the reliability of microbial electrolysis cells (MECs) in terms of recovering phosphorus as struvite from dewatering centrate and detecting organics in synthetic wastewater as bioanode sensors. However, there are still interesting aspects worth investigating in future work. Regarding phosphorus recovery, purity of the recovered struvite precipitants was not examined which could be affected by various operating conditions. Also, the reactor scale should be increased towards a practical application. In large scale reactor operation, long-term stability of the reactors needs to be verified. Moreover, hydrogen gas should be collected and quantified to estimate energy efficiency.

As for future bioanode sensor development, real wastewater such as primary clarifier effluent or anaerobic digester sludge should be tested. Stability of the long-term operation needs to be examined using real wastewater. Last but not least, the possibility of submersible reactor configurations should be investigated so that the sensors can become more applicable for real-time and in-situ monitoring of water quality in wastewater treatment and environmental engineering applications.

## References

- American Public Health Association, American Water Works Association & Water Environment Federation, 2012. *Standard methods for the examination of water and wastewater* 22nd ed. E. W. Rice et al., eds., American Water Works Assiation.
- Asztalos, J.R. & Kim, Y., 2015. Enhanced digestion of waste activated sludge using microbial electrolysis cells at ambient temperature. *Water Research*, 87, pp.503–512. Available at: <http://dx.doi.org/10.1016/j.watres.2015.05.045>.
- Baeza, M., Antonio, J. & Barcelona, D., 2016. Low-cost fuel-cell based sensor of hydrogen production in lab scale microbial electrolysis cells. , pp.2–9.
- Bond, P.L., Keller, J. & Blackall, L.L., 1999. Anaerobic phosphate release from activated sludge with enhanced biological phosphorus removal. A possible mechanism of intracellular pH control. *Biotechnol. Bioeng.*, 63(5), pp.507–15.
- Bridle, T.R. & Pritchard, D., 2004. Energy and nutrient recovery from sewage sludge via pyrolysis. *Water Science & Technology*, 50(9), pp.169–175.
- Burton, F. et al., 2013. *Wastewater Engineering: Treatment and Resource Recovery* 5th ed., McGraw-Hill Education.
- Cai, T., Park, S.Y. & Li, Y., 2013. Nutrient recovery from wastewater streams by microalgae: Status and prospects. *Renewable and Sustainable Energy Reviews*, 19, pp.360–369. Available at: <http://dx.doi.org/10.1016/j.rser.2012.11.030>.
- Cerrillo, M., Viñas, M. & Bonmatí, A., 2016. Removal of volatile fatty acids and ammonia recovery from instable anaerobic digesters with a microbial electrolysis cell. *Bioresource*



*Technology*, 219, pp.348–356.

- Chang, I.S. et al., 2004. Continuous determination of biochemical oxygen demand using microbial fuel cell type biosensor. *Biosensors and Bioelectronics*, 19(6), pp.607–613.
- Cheng, S. et al., 2009. Direct biological conversion of electrical current into methane by electromethanogenesis. *Environmental Science and Technology*, 43(10), pp.3953–3958.
- Colantonio, N. & Kim, Y., 2016. Cadmium (II) removal mechanisms in microbial electrolysis cells. *Journal of Hazardous Materials*, 311, pp.134–141. Available at: <http://dx.doi.org/10.1016/j.jhazmat.2016.02.062>.
- Cusick, R.D. et al., 2014. Electrochemical struvite precipitation from digestate with a fluidized bed cathode microbial electrolysis cell. *Water Research*, 54, pp.297–306. Available at: <http://dx.doi.org/10.1016/j.watres.2014.01.051>.
- Cusick, R.D. & Logan, B.E., 2012. Phosphate recovery as struvite within a single chamber microbial electrolysis cell. *Bioresource Technology*, 107, pp.110–115. Available at: <http://dx.doi.org/10.1016/j.biortech.2011.12.038>.
- Daigger, G.T. et al., 2011. *Biological Wastewater Treatment* 3rd ed., CRC Press.
- El Diwani, G. et al., 2007. Recovery of ammonia nitrogen from industrial wastewater treatment as struvite slow releasing fertilizer. *Desalination*, 214(1–3), pp.200–214.
- El-Shafai, S.A. et al., 2007. Nutrient recovery from domestic wastewater using a UASB-duckweed ponds system. *Bioresource Technology*, 98(4), pp.798–807.
- Fischer, F. et al., 2011. Microbial fuel cell enables phosphate recovery from digested sewage sludge as struvite. *Bioresource Technology*, 102(10), pp.5824–5830. Available at:

<http://dx.doi.org/10.1016/j.biortech.2011.02.089>.

Gilbert, N., 2009. Environment: The Disappearing Nutrient. *Nature*, 461(7265), pp.716–718.

Guest, J.S. et al., 2009. A New Planning and Design Paradigm to Achieve Sustainable Resource Recovery from Wastewater. *Environmental Science & Technology*, 43(16), pp.6126–6130.

Guo, K. et al., 2014. Surfactant treatment of carbon felt enhances anodic microbial electrocatalysis in bioelectrochemical systems. *Electrochemistry Communications*, 39, pp.1–4. Available at: <http://dx.doi.org/10.1016/j.elecom.2013.12.001>.

Hirooka, K. & Ichihashi, O., 2013. Phosphorus recovery from artificial wastewater by microbial fuel cell and its effect on power generation. *Bioresource Technology*, 137, pp.368–375. Available at: <http://dx.doi.org/10.1016/j.biortech.2013.03.067>.

Hrapovic, S. et al., 2010. Electrodeposition of nickel particles on a gas diffusion cathode for hydrogen production in a microbial electrolysis cell. *International Journal of Hydrogen Energy*, 35(14), pp.7313–7320. Available at: <http://dx.doi.org/10.1016/j.ijhydene.2010.04.146>.

Hu, H., Fan, Y. & Liu, H., 2009. Hydrogen production in single-chamber tubular microbial electrolysis cells using non-precious-metal catalysts. *International Journal of Hydrogen Energy*, 34(20), pp.8535–8542. Available at: <http://dx.doi.org/10.1016/j.ijhydene.2009.08.011>.

Ichihashi, O. & Hirooka, K., 2012. Removal and recovery of phosphorus as struvite from swine wastewater using microbial fuel cell. *Bioresource Technology*, 114, pp.303–307. Available at: <http://dx.doi.org/10.1016/j.biortech.2012.02.124>.

- Ichihashi, O., Tada, C. & Nakai, Y., 2011. Power Generation from Animal Wastewater Using Microbial Fuel Cell. *Journal of Integrated Field Science*, 8(November), pp.13–20.  
Available at: <http://ir.library.tohoku.ac.jp/re/bitstream/10097/50392/1/AA12005506-2011-8-13.pdf>.
- Iskander, S.M. et al., 2015. Resource recovery from landfill leachate using bioelectrochemical systems: Opportunities, challenges, and perspectives. *Bioresource Technology*, 201, pp.347–354. Available at: <http://dx.doi.org/10.1016/j.biortech.2015.11.051>.
- Jin, X. et al., 2016. Bio-electrolytic sensor for rapid monitoring of volatile fatty acids in anaerobic digestion process. *Water Research*, 111, pp.74–80. Available at: <http://dx.doi.org/10.1016/j.watres.2016.12.045>.
- Jouanneau, S. et al., 2014. Methods for assessing biochemical oxygen demand (BOD): A review. *Water Research*, 49(1), pp.62–82. Available at: <http://dx.doi.org/10.1016/j.watres.2013.10.066>.
- Karube, I. et al., 1977. Microbial electrode BOD sensors. *Biotechnology and Bioengineering*, 19(10), pp.1535–1547.
- Kaur, A. et al., 2014. Anode modification to improve the performance of a microbial fuel cell volatile fatty acid biosensor. *Sensors and Actuators, B: Chemical*, 201, pp.266–273.  
Available at: <http://dx.doi.org/10.1016/j.snb.2014.04.062>.
- Kaur, A. et al., 2013. Microbial fuel cell type biosensor for specific volatile fatty acids using acclimated bacterial communities. *Biosensors and Bioelectronics*, 47, pp.50–55. Available at: <http://dx.doi.org/10.1016/j.bios.2013.02.033>.

- Kumlanghan, A. et al., 2007. Microbial fuel cell-based biosensor for fast analysis of biodegradable organic matter. *Biosensors and Bioelectronics*, 22(12), pp.2939–2944.
- Larsen, T.A. et al., 2009. Source separation: Will we see a paradigm shift in wastewater handling? *Environmental Science & Technology*, 43(16), pp.6121–6125.
- Liberti, L. et al., 1981. Nutrient removal and recovery from wastewater by ion exchange. *Water Research*, 15(3), pp.337–342.
- Liu, H., Grot, S. & Logan, B.E., 2005. Electrochemically Assisted Microbial Production of Hydrogen from Acetate. *Environmental Science & Technology*, 39(11), pp.4317–4320.
- Logan, B.E. et al., 2008. Microbial Electrolysis Cells for High Yield Hydrogen Gas Production from Organic Matter. *Environmental Science & Technology*, 42(23), pp.8630–8640.
- Logan, B.E. et al., 2006. Microbial fuel cells: Methodology and technology. *Environmental Science and Technology*, 40(17), pp.5181–5192.
- Di Lorenzo, M. et al., 2009. A single-chamber microbial fuel cell as a biosensor for wastewaters. *Water Research*, 43(13), pp.3145–3154. Available at: <http://dx.doi.org/10.1016/j.watres.2009.01.005>.
- Maurer, M., Pronk, W. & Larsen, T.A., 2006. Treatment processes for source-separated urine. *Water Research*, 40(17), pp.3151–3166.
- Mavinic, D.S. et al., 1998. Anaerobic Co-Digestion of Combined Sludges from a Bnr Wastewater Treatment Plant. *Environmental Technology*, 19(1), pp.35–44. Available at: <http://www.tandfonline.com/doi/abs/10.1080/09593331908616653>.
- Merino Jimenez, I. et al., 2016. Enhanced MFC power production and struvite recovery by the

- addition of sea salts to urine. *Water Research*. Available at:  
<http://dx.doi.org/10.1016/j.watres.2016.11.017>.
- Modin, O. et al., 2012. Bioelectrochemical recovery of Cu, Pb, Cd, and Zn from dilute solutions. *Journal of Hazardous Materials*, 235–236, pp.291–297. Available at:  
<http://dx.doi.org/10.1016/j.jhazmat.2012.07.058>.
- Nancharaiah, Y.V., Venkata Mohan, S. & Lens, P.N.L., 2016. Recent Advances in Nutrient Removal and Recovery in Biological and Bioelectrochemical Systems. *Bioresource Technology*, 215, pp.173–185. Available at:  
<http://www.sciencedirect.com/science/article/pii/S0960852415008494>.
- Pinto, R.P. et al., 2010. A two-population bio-electrochemical model of a microbial fuel cell. *Bioresource Technology*, 101(14), pp.5256–5265.
- Qin, M. et al., 2016. Recovery of nitrogen and water from landfill leachate by a microbial electrolysis cell-forward osmosis system. *Bioresource Technology*, 200, pp.485–492.
- Quek, S.-B., Cheng, L. & Cord-Ruwisch, R., 2014. Detection of low concentration of assimilable organic carbon in seawater prior to reverse osmosis membrane using microbial electrolysis cell biosensor. *Desalination and Water Treatment*, 55(August 2015), pp.1–6. Available at:  
<http://www.tandfonline.com/doi/abs/10.1080/19443994.2014.940224>.
- Rittmann, B.E. & McCarty, P.L., 2012. *Environmental biotechnology: Principles and applications*, Tata McGraw Hill Education Private Limited.
- Ronteltap, M., Maurer, M. & Gujer, W., 2007. Struvite precipitation thermodynamics in source-separated urine. *Water Research*, 41(5), pp.977–984.

- Rozendal, R.A. et al., 2006. Principle and perspectives of hydrogen production through biocatalyzed electrolysis. *International Journal of Hydrogen Energy*, 31(12), pp.1632–1640.
- Rozendal, R.A. & Buisman, C.J.N., 2005. Process for Producing Hydrogen.
- Ryu, H.D., Kim, D. & Lee, S.I., 2008. Application of struvite precipitation in treating ammonium nitrogen from semiconductor wastewater. *Journal of Hazardous Materials*, 156(1–3), pp.163–169.
- Sakaguchi, T. et al., 2003. A rapid BOD sensing system using luminescent recombinants of *Escherichia coli*. *Biosensors and Bioelectronics*, 19(2), pp.115–121.
- Sakaguchi, T. et al., 2007. Rapid and onsite BOD sensing system using luminous bacterial cells-immobilized chip. *Biosensors and Bioelectronics*, 22(7), pp.1345–1350.
- Stein, N.E., Hamelers, H.V.M. & Buisman, C.N.J., 2012. Influence of membrane type, current and potential on the response to chemical toxicants of a microbial fuel cell based biosensor. *Sensors and Actuators, B: Chemical*, 163(1), pp.1–7. Available at: <http://dx.doi.org/10.1016/j.snb.2011.10.060>.
- Tice, R.C. & Kim, Y., 2014. Energy efficient reconcentration of diluted human urine using ion exchange membranes in bioelectrochemical systems. *Water Research*, 64, pp.61–72. Available at: <http://dx.doi.org/10.1016/j.watres.2014.06.037>.
- Torres, C.I., Kato Marcus, A. & Rittmann, B.E., 2007. Kinetics of consumption of fermentation products by anode-respiring bacteria. *Applied Microbiology and Biotechnology*, 77(3), pp.689–697.

- Udert, K.M. & Wächter, M., 2012. Complete nutrient recovery from source-separated urine by nitrification and distillation. *Water Research*, 46(2), pp.453–464.
- Wang, X. et al., 2009. Use of Carbon Mesh Anodes and the Effect of Different Pretreatment Methods on Power Production in Microbial Fuel Cells. *Environmental Science & Technology*, 43(17), pp.6870–6874.
- Yang, N., Hafez, H. & Nakhla, G., 2015. Impact of volatile fatty acids on microbial electrolysis cell performance. *Bioresource Technology*, 193, pp.449–455. Available at: <http://dx.doi.org/10.1016/j.biortech.2015.06.124>.
- Yang, W. et al., 2016. Fast and sensitive water quality assessment: A uL-scale microbial fuel cell-based biosensor integrated with an air-bubble trap and electrochemical sensing functionality. *Sensors and Actuators, B: Chemical*, 226, pp.191–195. Available at: <http://dx.doi.org/10.1016/j.snb.2015.12.002>.
- Yuan, Y. et al., 2016. Improving municipal wastewater nitrogen and phosphorous removal by feeding sludge fermentation products to sequencing batch reactor (SBR). *Bioresource Technology*, 222, pp.326–334. Available at: <http://linkinghub.elsevier.com/retrieve/pii/S0960852416313700>.
- Zhang, Y. & Angelidaki, I., 2012. A simple and rapid method for monitoring dissolved oxygen in water with a submersible microbial fuel cell (SBMFC). *Biosensors and Bioelectronics*, 38(1), pp.189–194. Available at: <http://dx.doi.org/10.1016/j.bios.2012.05.032>.
- Zhang, Y. & Angelidaki, I., 2014. Microbial electrolysis cells turning to be versatile technology: Recent advances and future challenges. *Water Research*, 56, pp.11–25. Available at: <http://dx.doi.org/10.1016/j.watres.2014.02.031>.

Zhang, Y. & Angelidaki, I., 2011. Submersible microbial fuel cell sensor for monitoring microbial activity and BOD in groundwater: Focusing on impact of anodic biofilm on sensor applicability. *Biotechnology and Bioengineering*, 108(10), pp.2339–2347.



## Appendix A: Additional files for Chapter 3



*Figure S 1 Dewatering centrate sample*

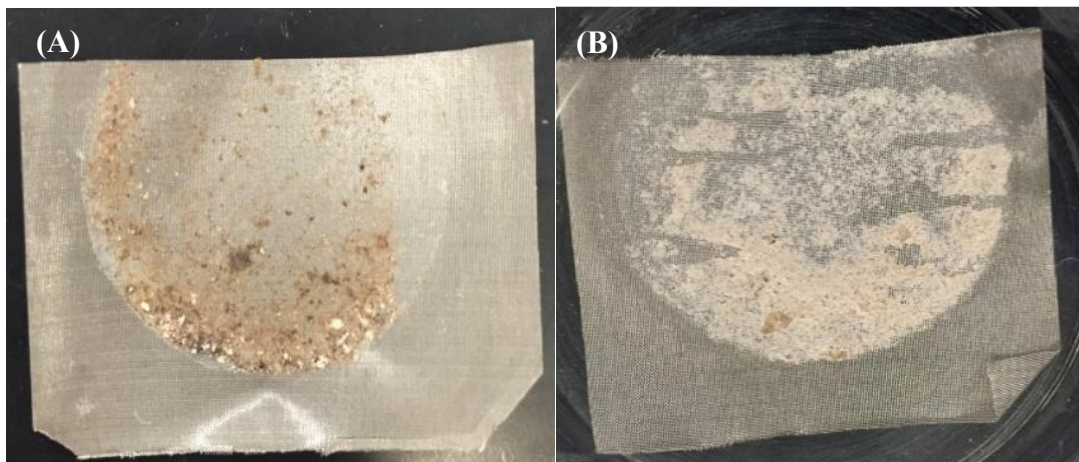


*Figure S 2 (A) SSM cathode image after controlled experiment (open circuit) with 2 mM magnesium and 4.5 mM phosphate addition. (B) SSM cathode image after one fed-batch SSM MEC operation with 4.5 mM phosphate addition for Set C*

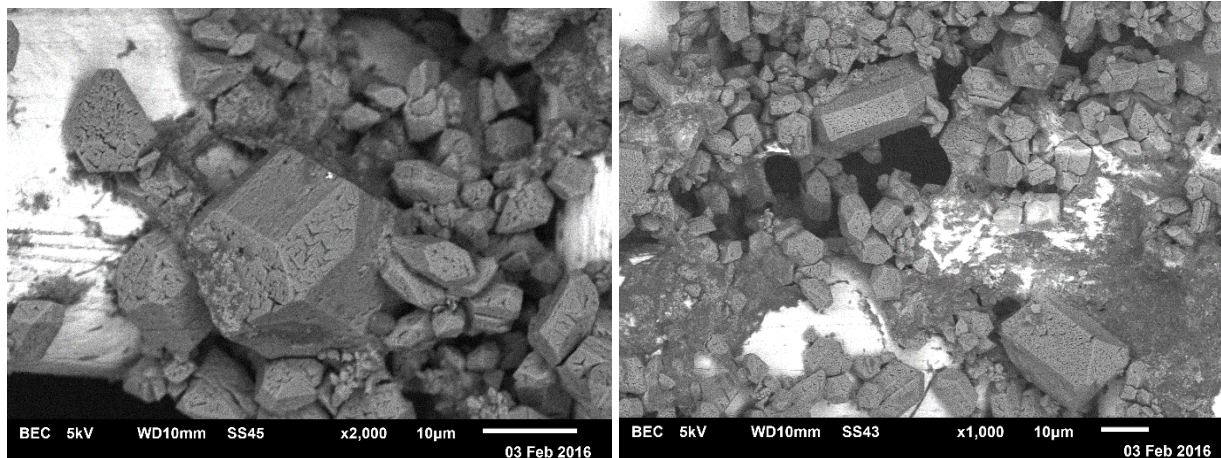


**Figure S 3** SEM images of struvite crystals on the SSM cathode after one fed-batch cycle (Set C with initial phosphate concentration of 3.26 mM)

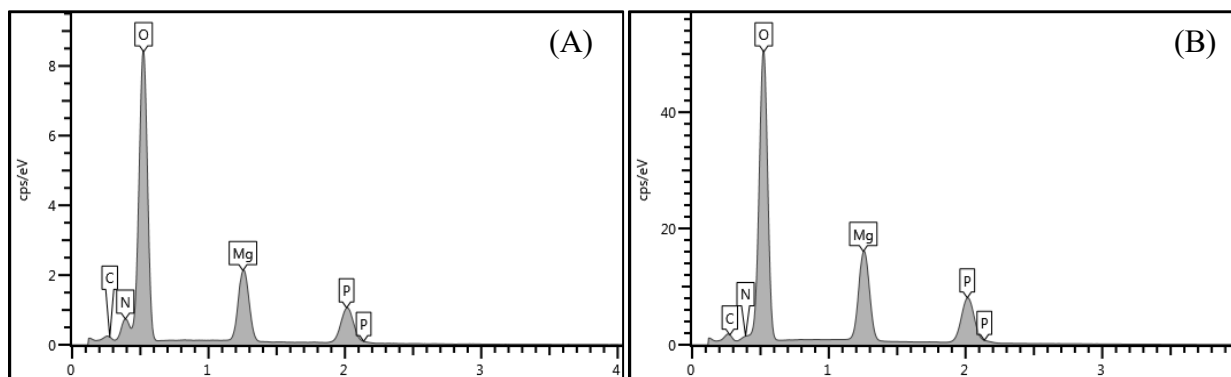


**Figure S 4** (A) EDS analysis results for the crystal on the SSM cathode. (B) EDS analysis results for pure struvite (99.999% purity)



*Figure S 5 SSF cathode image after 5-day fed-batch SSF MEC operation for Set D*

## **Appendix B: High current operation using a microcontroller**

### ***Introduction***

The main objective of this work was to maximize the electric current generation in an MEC fed with real wastewater without damaging the bioanode by high applied voltages. The new operation sequence developed in Chapter 4 was modified to monitor organic substrate levels and bioanode activities for enhanced electric current generation. The new operation sequence consists of three steps: Normal Operation that is dependent on the monitored information, Reset Step that removes the hysteresis effects, and Test Step that monitors the substrate content. The applied voltage ( $E_{ap}$ ) in the following Normal operation is adjusted based on the electric current at the end of Test Step. The applied voltage and electric current for each of the steps were controlled and monitored using a programmable logic controller (PLC).

## Methods

### Programmed logic description

1. Configure the pin resolutions ([Link](#)) and set the criteria and range of applied voltage
2. Apply operation sequences and record every 5 seconds (Figure S6)
3. Monitor the last recording of the Test Step
4. Change applied voltage based on the criterion
5. Loop step 2 to 4

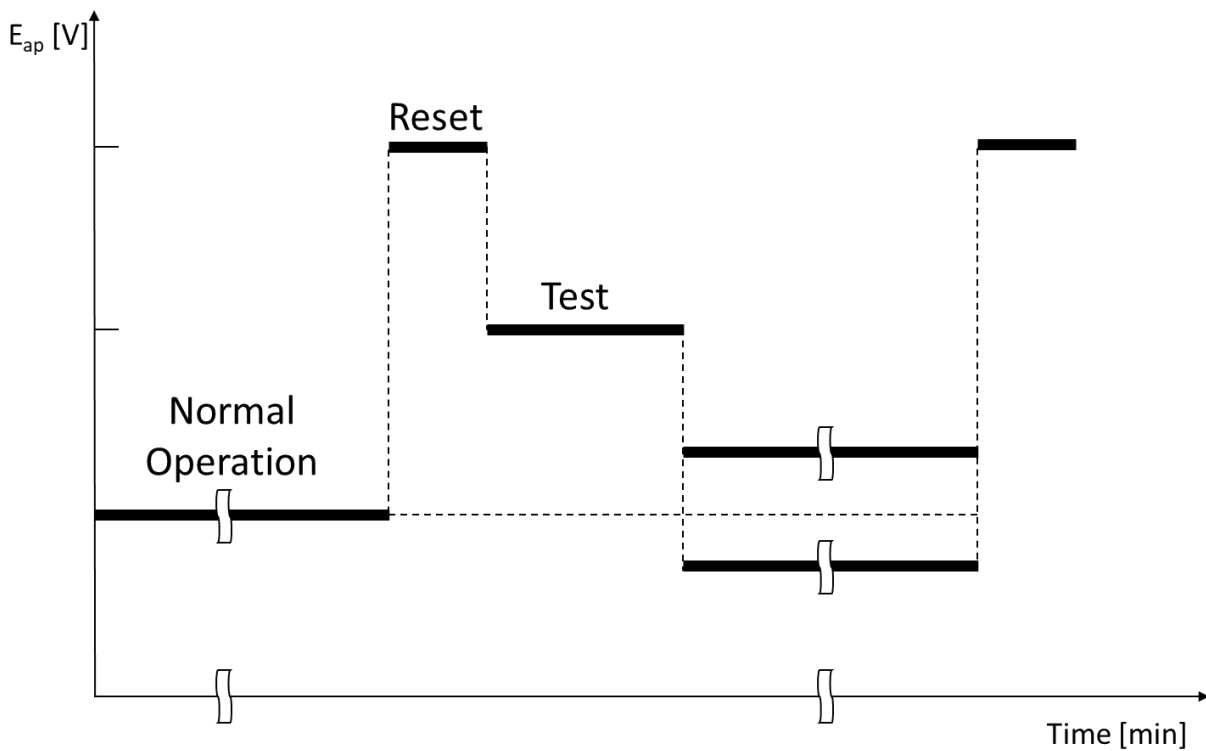
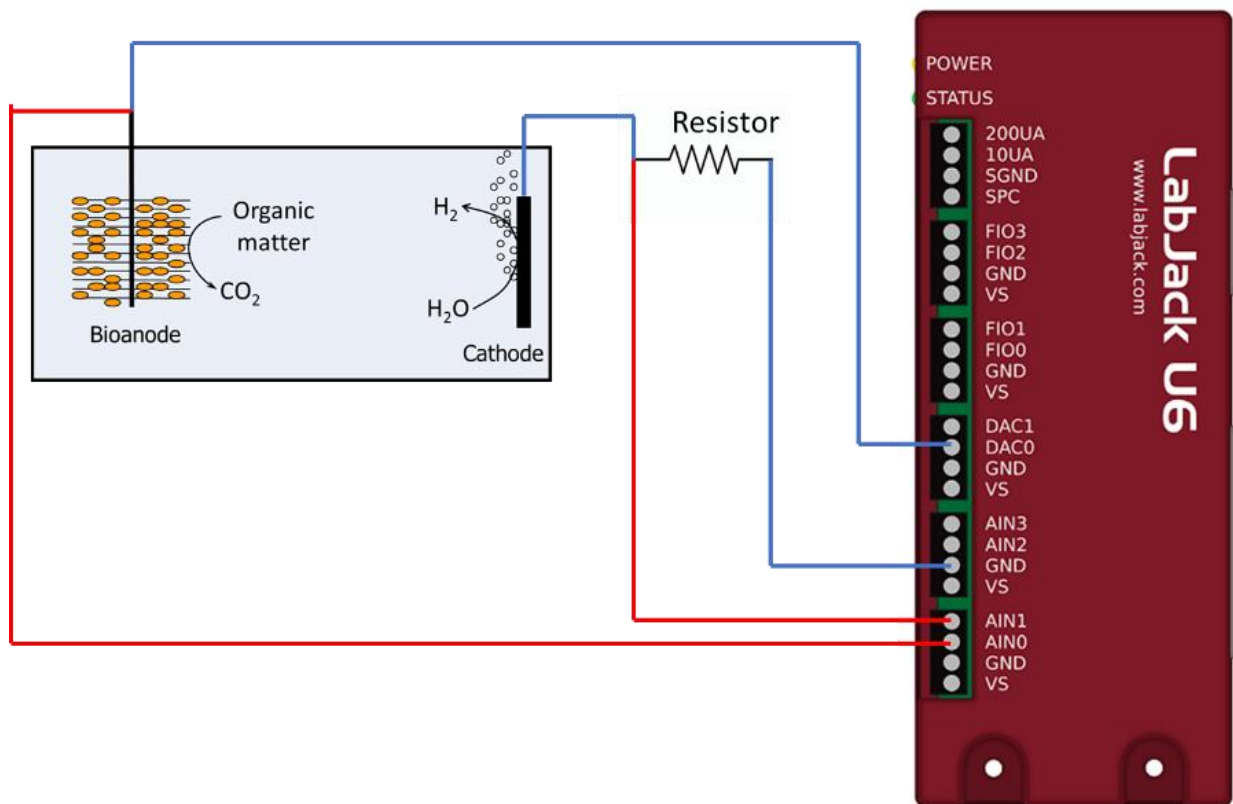


Figure S 6 Operation sequence

## Description of electric connections with PLC

- A commercial PLC (LabJack) was used in this study.
- DAC0 provides the applied voltage.
- AIN0 reads the total applied voltage.
- AIN1 reads the resistor voltage.



*Figure S 7 Connections of MEC and LabJack*

## Results

- Cycle duration was set to be 2 hr because of the lack of readily biodegradable substrates
- Electric current reached the steady state within 1 min during the Test Step
- Gain/Range of the pin used to read the voltage on resistor was set to be +/-1 volts  
(Resolution Index = 12). The resulting resolution was 0.7 uV.

| Duration of sequence | Duration of Reset Step | Criterion [mA] | E <sub>ap</sub> of Reset Step [V] | E <sub>ap</sub> of Test Step [V] | Results  |
|----------------------|------------------------|----------------|-----------------------------------|----------------------------------|--|
| 2hr                  | 15s                    | 0.01           | 1.8                               | 1.4                              | Highest E <sub>ap</sub> was 2.4V and highest I was ~0.5mA                |
| 2hr                  | 15s                    | 0.01           | 1.8                               | 1.4                              | Highest E <sub>ap</sub> was 2.8V and highest I was ~2.1mA; reactor fried |
| 2hr                  | 15s                    | 0.02           | 1.8                               | 1.4                              | E <sub>ap</sub> did not increase beyond 1.5V                             |
| 2hr                  | 15s                    | 0.025          | 1.8                               | 1.4                              | Highest E <sub>ap</sub> was 1.9V and highest I was ~0.13mA               |
| 2hr                  | 15s                    | 0.03           | 1.8                               | 1.4                              | Highest E <sub>ap</sub> was 1.7V and highest I was ~0.04mA               |
| 2hr                  | 15s                    | 0.05           | 1.8                               | 1.4                              | No E <sub>ap</sub> increase  |
| 2hr                  | 15s                    | 0.07           | 1.8                               | 1.4                              | No E <sub>ap</sub> increase  |

*Table S 1 Recent test results of examining primary clarifier effluents*